Effects of electron-phonon interaction in low-dimensional systems

A thesis submitted for the degree of

Doctor of Philosophy

by

Monisha P J

School of Physics
University of Hyderabad
Hyderabad-500046
India

Supervisor: Prof. Ashok Chatterjee

March 2016

To

My Parents

(Mr. John P T and Mrs. Mary John)

&

Husband

(Mr. Bibin P A)

Declaration

I, Monisha P J, hereby declare that the work presented in this thesis has been carried out by me under the supervision of Prof. Ashok Chatterjee, School of Physics, University of Hyderabad, Hyderabad, India, as per the Ph.D. ordinances of the University. I declare, to the best of my knowledge, that no part of this thesis has been submitted for the award of a research degree of any other University. I hereby agree that my thesis can be deposited in Shodhganga/INFLIBNET.

A report on plagiarism statistics from the University librarian is enclosed.

Monisha P J

Reg. No. 08PHPH13

Certificate

This is to certify that the thesis entitled **Effects of electron-phonon interaction in low-dimensional systems** being submitted to the University of Hyderabad by **Monisha P J** (Reg. No. 08PHPH13), for the award of the degree of Doctor of Philosophy in Physics, is a record of *bonafide* work carried out by her under my supervision and is free of plagiarism.

This matter embodied in this report has not been submitted to any other University or Institution for the award of any degree or diploma.

Prof. Ashok Chatterjee
Thesis supervisor,
School of Physics,
University of Hyderabad.

Dean
School of Physics,
University of Hyderabad.

Acknowledgements

First of all, I would like to thank my supervisor Prof. Ashok Chatterjee for accepting me as a PhD student and for his excellent guidance. His dedication to Physics has encouraged me to work sincerely and also, I thank him for making me a better human being.

I express my gratitude to Prof. Soma Mukhopadhyay for her wonderful support and suggestions. She has spent her valuable long hours for finding out the errors in my numerical calculations and was so patient to solve the problems. I thank her and Abhinava for being my good companions.

I thank Prof. Shreekantha Sil for the valuable suggestions and contributions to our works.

I am thankful to the doctorial committee members, Prof. S. Srinath and Dr. S.V.S. Nageswara Rao for their valuable suggestions. I thank Prof. Ashok Chatterjee, Prof. K P N Murthy and Prof. A. P. Pathak for their excellent lectures during the PhD course work.

I would like to express my sincere thanks to the former Deans of School of Physics, Prof. Vipin Srivatsava, Prof. C. Bansal Prof. S.P. Tewari and Prof. S. Chaturvedi. And finally, I thank the current Dean, Prof. R. Singh for providing the necessary facilities. I am grateful to the Directors and staff of the Centre for Modeling Simulation and Design (CMSD) for providing the computational facilities.

I thank Mr. T. Abraham and all other non-teaching staff of School of Physics for their help and support.

I express my sincere thanks to my colleagues I.V. Sankar, B. Aalu Naik, D. Sanjeev Kumar, Ch. Narasimha Raju, Luhluh Jahan and Ch. Uma Lavanya for their fruitful discussions and valuable suggestions.

I thank my friends Regina, Mini, Saipriya, Yasaswini, Siva, Balu, Suman, Vijayalakshmi, Jerin, Robin and my batch mates Sriramulu, Saikiran, Ahmed, RV, Sriram, Soorath and Sudhakar.

The financial assistance provided by University of Hyderabad and BSR fellowship of UGC is also greatly acknowledged.

I remember all my teachers and express my deep gratitude to them. Also, I would like to thank the principal Dr. Thomas Mathew and other staffs of St.Pius X college, Rajapuram.

I thank my parents for teaching me the greatness of educations and for their enormous support and sacrifices in fulfilling my dreams. Also, I thank my brother Jyothish and my sister Jomisha & her family for their love and encouragements. And I would like to thank my mother in law for her prayers and support. Also, I thank all the other family members and my friends.

Finally, I would like to thank my dear husband for his incessant encouragement and for being with me in crucial situations. My son Abraham also has to suffer a lot during my PhD period and his smile was the best solution for me to forget all my tensions.

Above all, I thank Almighty God for all the blessings in my life.

Monisha P J

Contents

Preface

Recent years have witnessed a flurry of investigations in the area of low-dimensional systems such as nano tubes, nano wires, quantum rings and quantum dots. Because of their nanoscale extensions in space, these systems have quantized energy spectra and exhibit many novel physical effects which are quite different from their bulk counterparts and are extremely interesting from the point of view of both fundamental physics and microelectronic device applications. The electron-phonon interaction has the same energy scale as the other relevant interactions in low-dimensional systems and it is therefore important to study the polaronic effects in these systems. Much effort has been directed towards exploring the polaronic properties of several low-dimensional systems and it has been observed in this connection that the polaronic effects can be very large if the sizes of these systems are reduced to a few nanometers. This thesis is an attempt to understand the effects of electron-phonon interactions in Luttinger liquid, correlated quantum ring and GaAs quantum dot.

First, we consider a one-dimensional (1D) electron system incorporating the electron-electron and electron-phonon interactions using the Luttinger model. We explicitly consider both the electron-optical-phonon interaction and the electron-acoustic-phonon interaction together with the electron-electron interaction. This system can be referred to as the Fr*ö*hlich-Toyozawa-Luttinger (FTL) liquid. We calculate the momentum distribution function of an FTL liquid exactly and examine how the momentum distribution function is affected by the electron-phonon interactions. Our results will be significant in the context of nanotubes and other systems where researchers have observed the Luttinger liquid behaviour experimentally.

Next we focus on a correlated quantum ring (QR) threaded by an Aharonov-Bohm (AB) flux where we study the effect of electron-phonon and Rashba spin-orbit (RSO) interactions on persistent current (PC). We use the Holstein-Hubbard-Rashba Hamiltonian for our calculations and also study the effect of temperature on PC. This work would be important in the emerging field of spintronics where RSO interaction is the key point.

We finally take up the problem of polaronic effect in a quantum dot (QD). It would be interesting in this context to study a polaronic effect which could be verified in the laboratory and the existence or otherwise of the polaronic effect can be tested experimentally. One of the polaronic effects that can be experimentally verified is the well-known pinning effect. We therefore study the pinning effect in a GaAs QD with Gaussian confining potential using the improved Wigner-Brillouin perturbation theory (IWBPT).

The thesis is based on the following publications.

1. **Monisha P.J**, S. Mukhopadhyay and A. Chatterjee, "Exact distribution function of a one-dimensional Frohlich-Toyozawa-Luttinger Liquid", *Solid State Communications* **166,** 83-86 (2013);

2. **Monisha P.J** and S. Mukhopadhyay, "The Pinning effect in a Gaussian quantum dot: A study using the Improved Wigner-Brillouin Perturbation theory", *Physica B* **464**, 38–43 (2015);

3. **Monisha P.J**, I.V. Sankar, S. Sil and A. Chatterjee, "Persistent Current in a Holstein-Hubbard Ring in the Presence of Rashba Spin Orbit Interaction", *Scientific Reports* **6**, 20056 (2016).

List of Figures

Chapter 1

Introduction

With the advent of modern sophisticated micro-fabrication techniques such as molecular beam epitaxy, nano-lithographic and etching techniques, organic chemical vapor deposition method, selective ion implantation and so on, it is now possible to realize ultra-low–dimensional structures such as thin films, quantum wells, nano tubes, quantum wires and polar semiconductor quantum dots in the laboratory. Naturally, extensive investigations [1] have been carried out both theoretically and experimentally in the last three decades on the low-dimensional systems. These studies are important to understand quite a few properties of matter which are exciting from the point of view of fundamental physics. It is possible to fabricate these nanosystems in different shapes and sizes which allow the researchers to manipulate their properties just by tuning the geometry of these systems. This design flexibility has given nano-materials an additional advantage for their application in micro-electronic devices such as single-electron transistors, quantum-dot lasers, quantum computers and so on. Because of the nanoscale dimension, the quantum characters dominate in low-dimensional systems and as a result they exhibit many physical properties which are quite different from those of their bulk counterparts.

In this thesis, we mainly focus on the effects of electron-phonon interaction on the electronic properties of low-dimensional systems like one-dimensional Luttinger liquids, Hubbard rings and quantum dots. It has

become, by now, well-known that the effects of electron-phonon interactions become more and more pronounced with the reduction in the dimensionality of the systems. Since we are interested in the one-dimensional (1D) and zero-dimensional (0D) systems here, let us look into the special features of those systems separately.

1.1 One-dimensional systems

The one-dimensional (1D) many-electron problem generated a lot interest after the discovery of quasi-one-dimensional organic solids like TTF-TCNQ in which the conductivity is thought to be largely 1D. In recent years the 1D systems attracted some renewed attention because of the possibility of realization of 1D nano-systems like carbon nanotubes and quantum wires. These correlated Fermi systems constitute an important area of research in solid state physics. The low-lying excited states of a strongly correlated system can be portrayed in terms of Bosonic collective excitations which are weakly interacting. Experiments on different materials have given the evidence that strong correlation functions are the key points to understand their physical properties.

The momentum distribution function is one of the best quantities to understand the many-body system. We know that a sharp discontinuity exists in the momentum distribution function of a non-interacting system. In the interacting systems also, one can define a Fermi surface in k-space as the locus of points where the momentum distribution is discontinuous. The Luttinger theorem states that the k-space volume enclosed by the Fermi surface defined by the discontinuity is unaffected by the interaction. The

systems which obey these assumptions are known as the normal Fermi systems and the interactions in these systems can be treated by the perturbation theory. But there are systems, in which the perturbative approach is not valid to study the interactions. *i.e*, the adiabatic continuity does not exist between the ground states of non-interacting and interacting systems. One of the examples is the 1D systems where the second order perturbative correction diverges logarithmically [2] and Landau's theory of Fermi liquid fails.

1.1.1 Fermi liquid theory

Landau's Fermi liquid theory describes an interacting Fermi system in terms of the fermionic quasiparticle. If we add an extra electron to an interacting Fermi system its mass and energy get modified. So the initially-bare electron is now dressed by the interaction and this dressed electron is an example of a fermionic quasiparticle. The main contribution of the interaction is taken into account by the mass renormalization. The low-lying states of the interacting system can be described as superpositions of quasiparticle excitations. We can talk about the quasiparticles only when a few of them are excited, otherwise the interaction among them also has to be considered. Hence the Fermi liquid theory will help us to understand the low-lying excited states near the Fermi surface. The quasiparticles possess the same quantum numbers as the original particles in the non-interacting case, but their dynamical properties are renormalized by the interactions and the corresponding operators commute with the Hamiltonian. We can treat the quasiparticle in the one-particle approximation. The energy of the quasiparticles in an unpolarized system is given by

$$\varepsilon_k = \mu + \frac{\hbar^2 k_F}{m^*}(k - k_F)\,. \tag{1.1}$$

where, k_F is the Fermi momentum and m^* is the effective mass. If we turn on the interaction in a non-interacting system after adding some electrons to the ground state, the same number of quasiparticles will be created. We define a smooth function δn_k by averaging over the neighboring $\boldsymbol{k}$ values and this function characterizes the excited states of both the free and the interacting system. The numbers δn_k are positive for $\boldsymbol{k}$ values lying outside the Fermi sphere and give the number of quasiparticles. The number of quasiparticle can be written as the difference,

$$\delta n_k = n_k - n_k^0 \tag{1.2}$$

where n_k and n_k^0 are the occupation number in the excited state and the ground state of the Fermi sea respectively and $n_k^0 = \theta(\mu - \epsilon_k)$, where μ is the chemical potential. The Landau theory is phenomenological which is based on the assumptions that the number of quasiparticles is small compared to the total number of particles. Assuming that there is no interaction between the quasiparticles the total energy of the system can be written as

$$E = E_0 + \sum_k \epsilon_k \, \delta n_k \tag{1.3}$$

where, E_0 is the ground state energy. We have to consider a grand canonical ensemble if the particle number is not conserved and the energy must be replaced by $E - \mu N_e$. Then, at finite temperature we write the free energy as

$$F = F_0 + \sum_k (\epsilon_k - \mu)\, \delta n_k \,. \tag{1.4}$$

where, F_0 is the free energy of the ground state. Till now, the explanation has been identical to that of a free Fermi system except for the effective mass. Eqn. (1.4) is linear in δn_k, but Landau has considered the weak interaction between the quasiparticles by taking the higher-order terms and suggested that we can terminate the expansion series in δn_k at the second order term, at low temperature

$$F = F_0 + \sum_k (\epsilon_k - \mu)\, \delta n_k + \frac{1}{2V} \sum_{kk'} f(k,k')\, \delta n_k \delta n_{k'} \,, \tag{1.5}$$

where $f(k,k')$'s are the Fermi liquid parameters or Landau parameters which characterize the interaction between quasiparticles. The quasiparticle concept is useful only if the life time is long enough and hence the idea of quasiparticle is valid only at low temperature and near Fermi surface and is appropriate to get the thermal and transport properties. The renormalized energy of the quasiparticle is the change in the free energy. We can determine the momentum distribution function of the quasiparticle using statistical mechanics and it is found that the usual Fermi-Dirac distribution function is restored with the renormalized energy states. These renormalized energies itself depend on the distribution function and hence we will have to calculate it self-consistently.

In normal metals, usually the electrons which are lying closer to the Fermi surface participate in most of the processes. So, the idea of quasiparticles and hence the Landau theory of Fermi

liquid is valid in metals [2]. In some systems where adiabatic continuity was absent initially, we can achieve it by reformulating the Hamiltonian and then can apply the Landau theory of Fermi liquids. If there is a finite gap in the excitation spectrum above the ground state of a quasiparticle, the system cannot be treated as a normal Fermi liquid.

1.1.2 Failure of Fermi liquid theory in one-dimension

In a 1D system the low-energy excitations are the electron-hole pairs which are bosonic elementary excitations and we do not have the fermionic quasiparticle in the system as such. The usual Fermi liquid theory based on quasiparticle picture breaks down in one-dimension because of the *Peierls instability* and *spin-charge separation*.

Peierls instability

The energy of the phonons gets modified by the electron-phonon interaction and the most interesting effects appear in the vicinity of $2k_F$. The derivative of the energy correction for general three-dimensional (3D) system exhibits a singularity at $2k_F$ at zero temperature. Therefore anomalous dispersion relation appears in the phonon energy at this wave number and is called Kohn anomaly. In 1D systems the energy correction itself shows a logarithmic singularity at $2k_F$ at low temperature and hence the anomaly is clearly visible here. Due to the $2k_F$ distortion of the lattice caused by the electron-phonon interaction, the unit cell gets doubled and the initially half filled band becomes completely filled in one-dimension. A gap forms at the zone boundary and the material becomes an insulator. This is known as the Peierls instability [3].

Spin-charge separation

In a 1D Fermi system the interactions involving spin and charge are different and a complete separation of the dynamics of the spin and charge degrees of freedom takes place and thus the charge and spin oscillations propagate with different velocities. So two distinctive excitations appear and this phenomenon is known as the spin-charge separation. Only for a non-interacting gas the two velocities are the same and equal to the Fermi velocity.

In a 1D chain, instead of the Fermi surface, we have just two Fermi points. Perfect nesting is possible in this case since one Fermi point can be translated into the other by a wavevector $\pm 2k_F$. This singular particle-hole type response is finite in Fermi liquid theory, but in one-dimension it is divergent and hence the Fermi liquid theory breaks down. Exact solutions are almost impossible for strongly interacting electron systems in higher dimensions, but there exist some models like Luttinger model and Hubbard model which are exactly soluble in one- dimension.

1.1.3 Luttinger Model

To study the spinless fermions in one dimension, Luttinger [4] proposed his model which is exactly solvable. The basic feature of the Luttinger model is that the system has two types of fermions which obey the linear dispersion relation as follows

Type - 1: $\epsilon_k = kv_F$; Type - 2: $\epsilon_k = -kv_F$,

and the two energy bands are independent. Consider the single-particle energy:

$$\epsilon_k = \frac{\hbar^2 k^2}{2m}\,. \tag{1.6}$$

Let $k = k_F + k'$, where k' is very small. Then we have

$$\frac{\hbar^2 k^2}{2m} = \frac{\hbar^2 (k_F + k')^2}{2m}\,. \tag{1.7}$$

When measured from the Fermi energy, we can write the energy as

$$\epsilon_{k'} = \frac{\hbar^2 (k_F + k')^2}{2m} - \frac{\hbar^2 k_F^2}{2m} = \frac{\hbar^2 k_F k'}{m}. \tag{1.8}$$

Writing k_F in terms of the Fermi velocity v_F, we get

$$\epsilon_{k'} = \hbar k' v_F\,. \tag{1.9}$$

We shall work in the Rydberg units and therefore we put $\hbar = 1$. Thus we get

$$\epsilon_k = k v_F\,, \tag{1.10}$$

which implies that the low-lying excitations in the case of the Luttinger model obey a linearized dispersion relation. It is assumed that the energy levels with negative energy are all filled up. Thus number of each type of particles is infinity. The Fermi surface for type - 1 particles is at wave vector $+k_F$ and for type - 2 particles it is at the negative wave vector $-k_F$. The energy spectrum of Luttinger model is given in Fig 1.1.

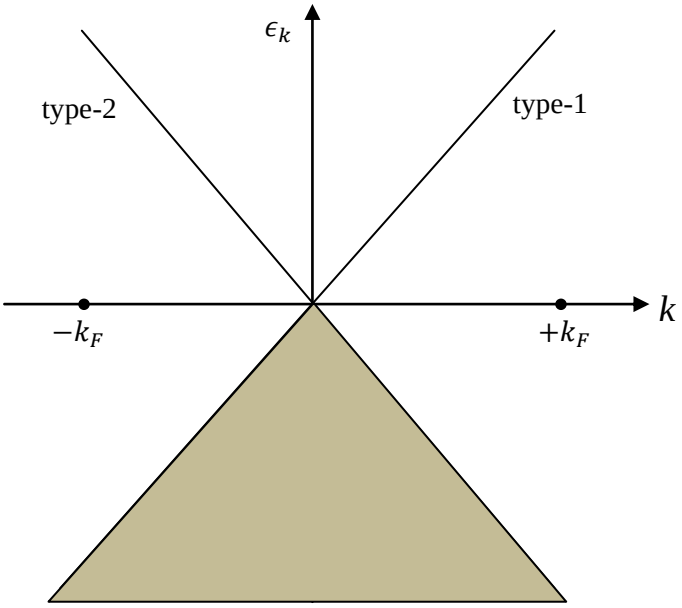

Fig 1.1: Linearized Dispersion curve of Luttinger model and the shaded portion is the filled negative energy states: Type – 1 : $\epsilon_k = +kv_F$; Type – 2 : $\epsilon_k = -kv_F$.

The basic model Hamiltonian for the Luttinger model is given by

$$H = H_0 + H' = \sum_k kv_F(a_{1k}^+ a_{1k} - a_{2k}^+ a_{2k}) + H' \qquad (1.11)$$

where $a_{1k}^+(a_{1k})$ and $a_{2k}^+(a_{2k})$ are the creation (annihilation) operators for the type - 1 and type - 2 fermions respectively and they satisfy the anti-commutation relations. H' is the interaction term. To solve the Hamiltonian, we define the density operators which can be expressed in terms of boson creation and annihilation operators. The Hamiltonian in terms of these bosonic operators becomes exactly solvable. Thus by using the bosonization technique the Luttinger Hamiltonian can be solved exactly. The Luttinger

model including the electron-electron interaction in one dimension is known as a Luttinger liquid.

Lieb and Mattis [5] have found that in a Luttinger liquid the Coulomb interaction removes the discontinuity but there still exists a *residual Fermi surface* at $k = k_F$. The electron-electron interaction term can be written in terms of the two density operators and the energy spectrum of the system is finally given by

$$\epsilon(k) = v_F|k|\left(1 + \frac{V_k}{\pi v_F}\right)^{1/2}, \tag{1.12}$$

where V_k is the Fourier transform of the electron-electron interaction potential i.e., the interaction in the momentum space.

The Luttinger model could be a suitable model for impurity problems or X-ray absorption problems in which the response of the electron gas to the central impulse can be factored into spherical harmonics associated with different angular momentum states *l*. Each angular momentum channel then becomes a 1D electron gas to which this model can be applied. The Luttinger liquid behaviour has indeed been observed experimentally in carbon nanotubes and other quasi-one-dimensional conductors [6].

1.1.4 Hubbard Model

The Hubbard model is one of the simplest models for the interacting electrons. In the Hubbard model the hopping term gets its maximum contribution from the nearest neighbour (NN) lattice points and the interaction between the electrons on the same site is taken into account. The Hubbard model is exactly solvable only in one-dimension. With the

assumption that the electrons can hop only to the NN sites, the Hubbard Hamiltonian can be written as

$$H = \varepsilon_0 \sum_{i\sigma} c_{i,\sigma}^{\dagger} c_{i,\sigma} - t \sum_{\langle ij\rangle,\sigma} \left[c_{i,\sigma}^{\dagger} c_{j,\sigma} + h.c\right] + U \sum_{i} n_{i\uparrow} n_{i\downarrow} \,, \qquad (1.13)$$

where the first term represents is the site energy, ε_0 being the onsite energy and $c_{i,\sigma}^{\dagger}(c_{i,\sigma})$ the creation (annihilation) operator for an electron at site i with spin σ . The second term is the kinetic energy term, t giving the hopping amplitude and the notation $\langle ij\rangle$ implying that the summation is to be performed over the NN sites i and j. The third term describes the onsite coulomb repulsion term with U as the strength of the interaction and $n_{i\sigma} = c_{i\sigma}^{\dagger} c_{i\sigma}$ the number operator for the electrons at site i with spin σ. In the absence of the onsite Coulomb repulsion, the unperturbed energy is given by

$$E = -2t \sum_{j=1}^{N_e} cos\left(k_j a\right) \qquad (1.14)$$

where the summation is over the occupied one-particle states. For simplicity we take $a = 1$ and the number of electrons less than or equal to the number of lattice sites. Also, we assume that the system can be at most half filled and the energy takes the same form as that of the non-interacting system provided the values of the wave numbers are modified. Lieb and Wu [7] have exactly solved the 1D Hubbard Hamiltonian for the first time, using the Bethe ansatz. In the extended Hubbard model we include also the interaction between the electrons at the nearest neighbor sites. Adding the electron-phonon interaction to this Hamiltonian one gets the so called the Holstein-Hubbard [8] Hamiltonian, a detailed discussion of which is given in Section 1.3. To study the effects of spin-orbit interaction [9] in quantum

rings, one has to add the spin-orbit interaction term to the Holstein-Hubbard Hamiltonian. In the present thesis we are interested in a quantum ring with a finite number of sites in the presence of both electron-phonon and electron-electron and spin-orbit interactions. Thus the Holstein-Hubbard model with a spin-orbit interaction term is the most suitable model for this system.

1.2 Zero-dimensional systems (Quantum dots)

Quantum dots (QD's) are ultrasmall structures in which the motion of the charge carriers is confined in all spatial directions. A QD contains a finite number of electrons and the energy levels are discrete. When the electrons are confined to length scales smaller than the electron wavelength, the quantum mechanical effects dominate in the system. Interest in the subject of QD has continued unabated for the last three decades mainly for two reasons. First and foremost, quantum dots provide an excellent laboratory where the predictions of quantum mechanics can be tested. Secondly and probably more importantly, QD's exhibit very many novel physical properties which are quite different from those of their bulk counterparts [10] and have tremendous potentiality for applications [11] in nano-electronic technology, opto-electronic devices, quantum transport at nano-scale, spintronics and biological systems.

To study the properties of a QD theoretically, it is required to prescribe an attractive model potential to describe the quantum confinement. Initial studies have considered square well potential models to simulate a QD [12]. However, some magneto-optical experiments [13, 14] have shown that the resonance frequencies of QD's are independent of the number of electrons

in the dot. These observations together with the generalized Kohn theorem [15] suggest that the confining potential in a QD is more or less parabolic. This has led to a host of investigations on parabolic QD's [16]. Later experiments have suggested that the confining potential in a QD is anharmonic in nature and Adamowsky et al. [17] have used an attractive Gaussian confining potential (GCP) to successfully explain some QD properties. We would like to mention in passing that the Gaussian potential has proved to be a useful potential in various branches of physics and has been solved approximately for a single-particle problem by several authors [18].

1.3 Effects of electron-phonon interactions

The electron-phonon interaction in polar materials produces quasi-particles called polarons. The Frohlich single polaron model [19] which totally neglects the electron-electron interaction works well for systems in which the carrier density is low. However if the carrier concentration is large, we cannot ignore the interaction between the electrons. In the tight-binding model, the polarons are best described by the Holstein model [20]. The observation of high-temperature superconductivity in 1D systems has motivated the researchers to study the electron-phonon interaction in these systems. There have been many investigations [21] to study the effect of electron-phonon interaction in the Luttinger model. These studies can also shed light on the interplay between the electron-phonon and electron-electron interactions. In this thesis, we are interested in the polaronic effects in a correlated 1D system in the continuum model where we include interaction of the electrons with both optical and acoustic phonons.

The most suitable model to study the interplay between the electron-phonon interaction and the Coulomb repulsion in narrow-band systems is the Holstein-Hubbard (HH) model [8]. Cabib and Callen [22] have shown that the spin order and the charge order do not co-exist. However, a deeper and more careful look suggests that there could be yet another effect arising due to the competition between the phonon induced attractive interaction between electrons and the direct Coulomb repulsion which might lead to some kind of a compromise at the crossover region so much so that the transition from one insulating state to the other may not be direct as normally believed but may go through an intermediate phase and it is this phase which will be the subject of our interest. Several studies [23] on the HH model have revealed that it can afford interesting phase diagrams due to the competition among charge-density wave (CDW), spin-density wave (SDW), and superconductivity as we change the parameters involved in the system. Recently, Takada and Chatterjee [24] have shown for the first time within the framework of 1D HH model at half-filling that there may exist an intervening phase at the CDW-SDW crossover region and, interestingly enough, this phase is metallic. This theoretical observation is of great importance because such a metallic state, if exists, would be just ideal for high-temperature superconductivity. We study in this thesis the electron-phonon, electron-electron and the spin-orbit interaction effects in a quantum ring using the Holstein-Hubbard model with a spin-orbit interaction term.

In QD's, the electron–phonon interaction energy scale is almost comparable to the confinement energy and electron correlation energy. So, it is essential to study the effect of electron-phonon interaction on the electronic properties of a QD. Most of the QD's available today are made of

polar semiconductors, in which the electron-phonon interaction will lead to the formation of polarons. A number of studies [25] have predicted several polaronic effects in polar semiconductor QD's and these effects will influence the transport and optical properties of a QD. Schmitt-Rink et al. [26] have predicted a weak phonon broadening of the linear spectrum lines in the limit of QD. Later, Bockelmann and Bastard [27] have studied the same in a QD. Zhu and Gu [28] have calculated certain polaronic properties using the second order perturbation theory. Mukhopadhyay and Chatterjee [29] have calculated the polaronic correction to the ground and first excited states of an electron in a QD using perturbation theory. They have also calculated the polaron self-energy by a variational method [30] and studied the formation and stability of bipolarons in QD's [31]. They have furthermore studied the magnetopolaron problem in which they have predicted the suppression of Zeeman splitting in a GaAs QD [32]. Koch et al. [33] have performed a Green's function-based calculation to study the effects of electron-phonon coupling on transport through a molecular QD in the quantum limit. These polaronic effects are size dependent and hence we can control them. In the present thesis we shall study the well-known polaronic effect called the pinning effect in a quantum dot with Gaussian confinement. This is an observable effect and can be used to verify the existence or otherwise of the polaronic effect in a QD.

1.4 Organization of the thesis

In the chapter immediately following i.e., in **Chapter 2**, we obtain an exact analytical expression for the electron momentum distribution function of a 1D interacting electron problem within the framework of

Luttinger model incorporating both the electron-optical-phonon interaction and the electron-acoustic-phonon interaction along with the electron-electron interaction. We refer this system as the Fr*ö*hlich-Toyozawa-Luttinger (FTL) liquid. It is explicitly shown that the residual Fermi surface disappears when the electron-electron interaction is increased and the electron-phonon interactions also flatten the distribution function. However, it is found that the nature of the distribution function of an FTL liquid is qualitatively different from that of the corresponding Luttinger liquid above k_F.

In C**hapter 3,** the persistent current in a correlated quantum ring threaded by an Aharonov-Bohm flux is studied in the presence of electron-phonon interactions and Rashba spin-orbit coupling. The quantum ring is modeled by the Holstein-Hubbard-Rashba Hamiltonian and the energy is calculated. The effects of Aharonov- Bohm flux, temperature, chemical potential spin-orbit interaction and electron-phonon interaction on the persistent current are investigated. It is shown that the electron-phonon interactions reduce the persistent current, while the Rashba coupling enhances it. It is also shown that temperature smoothens the persistent current curve.

Chapter 4 describes the pinning of the excited energy levels to the ground state plus one phonon energy in a Gaussian quantum dot in the presence of electron-phonon interaction. The calculation is performed using the improved Wigner-Brillouin perturbation theory (IWBPT). The electron-phonon interaction lifts the degeneracy present in the unperturbed problem and consequently, the excited energy levels bend and get pinned to the ground state plus one phonon state as we increase

the confinement frequency. The effect of different confining potentials are also been discussed.

Finally, in **Chapter 5** we summarize the important results of this thesis and present our conclusions.

References

[1] J. Lee and H. N. Spector, *J. Appl. Phys.* **54**, 3921(1983); *ibid*. **57**, 366 (1985);
J. Lee and M. O. Vassell, *J. Phys. C* **17**, 2525 (1984);
J. P. Leburton, *J. Appl. Phys.* **56**, 2850 (1984);
S. S. Kubakaddi and B. G. Mulimani, *J. Phys. C* **18**, 6647 (1985);
M. H. Degani and O. Hipolito, *Phys. Rev. B* **35**, 9345 (1987);
M. H. Degani and O. Hipolito, *Solid State Commun.* **65**, 1185 (1988);
P. Roussignol, D. Ricard and C. Flytzanis, *Phys. Rev. Lett.* **62**, 312 (1989);
C. Quinghu, R. Yuhang, T. Li, Y. Yabin and Z. Jiao, *J. Phys.: Condens. Matter* **11**, 4189 (1999);
F. Buonocore, G. Iadonisi, D. Ninno and F. Ventriglia, *Phys. Rev. B* **65**, 205415 (2002);
H. Xie, *Physica E* **22**, 906 (2004);
W. S. Li, S. W. Gu, T. C. Au-Yeung and Y. Y. Yeung, *Phys. Rev. B* **46**, 4630 (1992);
T. Yildirim and A. Ercelebi, *J. Phys.: Condens. Matter* **3**, 1271 (1991);
H. Y. Zhou and S. W. Gu, *Solid State Commun.* **91**, 725 (1994);
Y. H. Ren *et al.*, *Eur. Phys. J. B* **7**, 651 (1999);

P. M. Krishna and A. Chatterjee, *Physica B* **358**, 191 (2005);

S. K. Yip, *Phys. Rev.* B **43** 1707 (1991);

M. Henini, S. P. Beaumont and C. D. W. Wilkinson, *Phys. Rev. Lett.* **68**, 1754 (1992);

S. W. Gu and K. X. Guo, *Solid State Commun.* **89**, 1023 (1993);

K. D. Zhu and S. W. Gu, *Phys. Lett.* A **172**, 296 (1993);

C. Sikorski and U. Merkt, *Phys. Rev. Lett.* **62**, 2164 (1989);

L. E. Burs, *J. Chem. Phys.* **80**, 4403 (1984);

V. Halonen, T. Chakraborty and P. Pietilainen, *Phys. Rev.* B **45**, 5980 (1992);

G. W.Bryant, *Phys. Rev. Lett.* **59**, 1140 (1987);

G. W.Bryant, *Phys. Rev.* B **37**, 8763 (1988);

G. W.Bryant, *Phys. Rev.* B **41**, 1243 (1990);

U. Merkt, J. Huser and M. Wagner, *Phys. Rev.* B **43**, 7320 (1991);

J. Y. Marzin and G. Bastard, *Solid State Commun.* **92**, 437 (1994);

B. Boyacioglu and A. Chatterjee, Int. J. Mod. Phys. B **26**, 1250018 (2012).

[2] J. Solyom, *Fundamentals of the Physics of Solids*, Volume III: Normal, Broken-Symmetry, and Correlated Systems;

H. Bruus and K. Flensberg, *Introduction to Many-body quantum theory in condensed matter Physics;*

G. D. Mahan, *Many-Particle Physics*;

J. Voit, *Rep. Prog. Phys.* **58**, 977 (1995), *One dimensional Fermi liquids.*

[3] W. Kohn, *Phys. Rev. Lett.* **2**, 393 (1959);

R. E. Peierls, *Quantum Theory of Solids* Oxford University, Oxford, (1955).

[4] J. M. Luttinger, *J. Math. Phys.* **4**, 1154 (1963).

[5] D. C. Mattis and E. H. Lieb, *J. Math. Phys.* **6**, 304 (1965).

[6] M. Bockrath *et al.*, *Nature* **397**, 598 (1999);
M. Sing *et al.*, *Phys. Rev. B* **68**, 125111 (2003);
S. Sen and S. Chakrabarti, *Physica E* **40,** 2736 (2008).

[7] E. H. Lieb and F. Y. Wu, *Phys. Rev. Lett.* **20**, 1445 (1968).

[8] A. N. Das and S. Sil, *Physica C* **161**, 325 (1989);
E. Berger, P. Valasek and W. von der Linden, *Phys Rev B*, **52**, 4806 (1995);
S. Sil and B. Bhattacharyya, *Phys. Rev. B* **54**, 14349 (1996);
C. H. Pao and H. B. Schuttler, *Phys. Rev. B* **57**, 5051 (1998);
A.Weiße, H. Fehske, G.Wellein and A. R. Bishop, *Phys. Rev. B* **62**, R747 (2000);
V. Cataudella, G. De Filippis and G. Iadonisi, *Phys. Rev. B* **62**, 1496 (2000);
W. Koller, A. C. Hewson and D. M. Edwards, *Phys. Rev. Lett.* **95**, 256401 (2005);
G. Sangiovanni, M. Capone, C. Castellani and M. Grilli, *Phys. Rev. Lett.* **94**, 026401 (2005);
P. Barone, R. Raimondi, M. Capone and C. Castellani, *Phys. Rev. B* **73**, 085120 (2006);
Y. Takada, *J. Phys. Soc. Jpn*. **65**, 1544 (1996);
E. Jeckelmann, C. Zhang and S. R. White, *Phys. Rev. B* **60**, 7950 (1999);
Q. Wang, H. Zheng, and M. Avignon, *Phys. Rev. B* **63**, 014305 (2000).

[9] T. Koga, J. Nitta, T. Akazaki and H. Takayanagi, *Phys. Rev. Lett.* **89**, 046801 (2002);
J. Premper, M. Trautmann, J. Henk and P. Bruno, *Phys. Rev. B* **76**, 073310 (2007);

S. Sil, S. K. Maiti and A. Chakrabarti, *J. Appl. Phys.* **112**, 024321 (2012);

S. K. Maiti, M. Dey, S. Sil, A. Chakrabarti and S. N. Karmakar, *Europhys. Lett.* **95**, 57008 (2011).

[10] P. Moriarty, *Rep. Prog. Phys.* **64**, 297 (2001).

[11] M. A. Kastner, *Rev. Mod. Phys.* **64**, 849 (1992);

N. F. Johnson, *J. Phys.: Condens. Matter* **7**, 965 (1995);

R. C. Ashoori, *Nature* **379**, 413 (1996);

U. Woggon, *Optical Properties of Semiconductor Quantum Dots* (Springer, Berlin, 1997);

L. Jack, P. Hawrylack and A. Wojs, *Quantum Dots* (Springer, Berlin, 1998);

D. Bimberg, M. Grundmann and N. N. Ledentsov, *Quantum Dot Heterostructures* (Wiley, New York, 1998).

[12] F. Geerinckx, F. M. Peeters and J. T. Devreese, *J. Appl. Phys.* **68**, 3435 (1990);

J.-L. Zhu, J.-J. Xiong and B.-L. Gu, *Phys. Rev. B* **41**, 6001(1990);

T. Takagahara *Phys. Rev. B* **47**, 4569 (1993);

N. Porras-Montenegro, S. T. Perez-Merchancano and A. Latge, *J. Appl. Phys.***74**, 7624 (1993);

J. L. Marín, R. Riera and S. A.Cruz, *J. Phys. Condens. Matter* **10**, 1349 (1998).

[13] Ch. Sikorski and U. Merkt, *Phys. Rev. Lett.* **62**, 2164 (1989); *ibid. Surf. Sci*. **229**, 282 (1990);

B. Meurer, D. Heitmann and K. Ploog, *Phys. Rev. Lett.* **68**, 1371(1992);

R. C. Ashoori *et al.*, *Phys. Rev. Lett*. **68**, 3088 (1992);

H. Drexler, D. Leonard, W. Hansen, J. P. Kotthaus and P. M. Petroff, *Phys. Rev. Lett.* **73**, 2252 (1994).

[14] F. M. Peeters, *Phys. Rev. B* **42**, 1486 (1990);
S. K. Yip, *Phys. Rev. B* **43**, 1707 (1991);
Q.P. Li, K. Karrai, S. K. Yip, S. Das Sarma and H.D. Drew, *Phys. Rev. B* **43**, 5151 (1991).

[15] W. Kohn, *Phys. Rev.* **123,** 1242 (1961).

[16] P. A. Maxym and T. Chakraborty, *Phys. Rev. Let*t. **65**, 108 (1990);
N. F. Johnson and M. C. Payne, *Phys. Rev. Lett.* **67**, 1157 (1991);
N. F. Johnson and F. C. Payne, *Phys. Rev. B* **45**, 3819 (1992);
R. Egger, W. Hausler, C.H. Mak and H. Grabert, *Phys. Rev. Lett.* **82**, 3320 (1999);
L. Lu, W. Xie and S. Liang, *Curr. Appl. Phys.* **11**,1302 (2011).

[17] J. Adamowsky, M. Sobkowicz, B.Szafran and S.Bednarek, *Phys. Rev. B* **62**, 4234 (2000).

[18] N. Bessis, G. Bessis and B. Joulakian, *J. Phys. A: Math. Gen.* **15**, 3679 (1982);
C. S. Lai, *J. Phys. A: Math. Gen.* **16**, L181 (1983);
R. E. Crandall, *J. Phys. A: Math. Gen.* **16**, L395 (1983);
M. Cohen, *J. Phys. A: Math. Gen.* **17**, L101 (1984);
A. Chatterjee, *J. Phys. A: Math. Gen.* **18**, 2403 (1985);
A. Chatterjee, *Phys. Rep.* **186**, 249 (1990).

[19] H. Fröhlich, *Phil. Mag. Suppl.* **3**, 325 (1954).

[20] T. Holstein, *Annals of Physics* **8**, 325 (1959).

[21] I. Baldea, *Physica Scripta* **31**, 606 (1985).
E. C. Marino, *Phys. Rev. Lett.* **55**, 2991 (1985);
M. J. Martins, *J. Phys. C* **20**, L765 (1987);
C. S. Rao, P. M. Krishna, S. Mukhopadhyay and A. Chatterjee, *J.*

Phys.: Condens. Matter **13**, L919 (2001).

[22] D. Cabib and E. Callen, *Phys. Rev. B* **12**, 5249 (1975).

[23] A. Chatterjee and Y. Takada, *J. Phys. Soc. Jpn*. **73**, 964 (2004);
P. M. Krishna and A. Chatterjee, *Physica C* **457**, 55 (2007).

[24] Y. Takada and A. Chatterjee, *Phys. Rev. B* **67**, 081102 (R) (2003).

[25] J.S. Pan and B.H. Pan, *Phys. Status Sol. (b)* **148**, 129 (1988);
S.K. Yip, *Phys. Rev. B* **40**, 3682 (1989);
M. C. Klein, E. Hache, D. Ricard and C. Flytzanis, *Phys. Rev. B* **42**, 11123 (1990);
M. G. Bawendi *et al.*, *Phys. Rev. Lett.* **65**, 1623 (1990);
S. Nomura and T. Kobayashi, *Phys. Rev. B* **45**, 1305 (1992);
L. Wendler, A. V. Chaplik, R. Haupt and O. Hipolito, *J. Phys. Condens. Matter* **5**, 8031 (1993);
S. Sahoo, *Z. Phys. B* **101** 97 (1996)
C. Y. Chen, P. W. Jin, W. S. Li and D. L. Din, *Phys. Rev.* **56**, 14913 (1997);
M. A. Odnoblyudov, I. N. Yassievich and K. A. Chao, *Phys. Rev. Lett.* **83,** 4884 (1999);
N. Kervan, T. Altanhan and A. Chatterjee, *Phys. Lett. A* **315**, 280 (2003).

[26] S. Schmit-Rink, D. A. B. Miller and D. S. Chemla, *Phys. Rev. B* **35,** 8113 (1987).

[27] U. Bockelmann and G. Bastard, *Phys. Rev. B* **42**, 8947 (1990).

[28] K. D. Zhu and S. W. Gu, *Phys. Lett. A* **163**, 435 (1992)
K. D. Zhu and S. W. Gu, *J. Phys. Condens. Matter* **4**, 1291 (1992).
K. D. Zhu and S. W. Gu, *Phys. Rev. B* **47**, 12947 (1993);
K. D. Zhu and T. Kobayashi, *Solid State Comm*. **92**, 353 (1994).

[29] S. Mukhopadhyay and A. Chatterjee, *Phys. Lett. A* **204**, 411 (1995);

S. Mukhopadhyay and A. Chatterjee, *Phys. Lett. A* **240**, 100 (1998).

[30] S. Mukhopadhyay and A. Chatterjee, *Phys. Rev. B* **58**, 2088 (1998);
S. Mukhopadhyay and A. Chatterjee, *J. Phys.: Condens. Matter* **11**, 2071 (1999);
A. Chatterjee and S. Mukhopadhyay, *Acta Phys. Pol B* **32**, 473 (2001).

[31] S. Mukhopadhyay and A. Chatterjee, *J. Phys. Condens. Matter* **8**, 4017 (1996);
P.M. Krishna, S. Mukhopadhyay and A. Chatterjee, *Phys. Lett. A* **360**, 655 (2007).

[32] A. Chatterjee and S. Mukhopadhyay, *Phys. Rev. B* **59**, R7833 (1999);
S. Mukhopadhyay and A. Chatterjee, *Int. J. Mod. Phys. B* **14**, 3897 (2000).

[33] T. Koch, J. Loos, A. Alvermann, A. R. Bishop and H. Fehske, *Journal of Physics: Conference Series* **220**, 012014 (2010).

Chapter 2

Exact distribution function of a Luttinger Liquid in the presence of electron-phonon interaction

2.1 Introduction

The Luttinger model is an exactly solvable model proposed by Luttinger [1] to study the one-dimensional (1D) many-fermion systems. This problem has achieved its importance in recent years after the discovery of carbon nanotubes, quantum wires and other quasi-one-dimensional organic solids such as TTF-TCNQ and the experimental observation of Luttinger liquid (LL) behavior in these systems [2]. The edge excitation states of a quantum Hall conductor are also an example of a LL.

The concept of Luttinger liquids became more popular after Anderson's observation that the normal state properties of the two-dimensional (2D) high-temperature superconductors are more similar to that of a LL [3]. Anderson proposed that the essential physics of these new superconductors is contained in the 2D Hubbard model and suggested a tomographic LL picture for the ground state and the low-energy excitations of this model. This proposal was based on the assumption that the Hubbard model in one and two dimensions has a somewhat similar behavior and shows the LL behavior for a certain range of the parameters. The 1D electron-phonon systems or metals with impurities can also be LL's.

Bloch [4] suggested in his paper that 1D non-interacting fermions have the same type of low-energy excitations as a harmonic chain. Tomonaga [5] used Bloch's method to study the interacting fermions and solved the 1D interacting fermion problem exactly for the first time, using bosonization and certain approximations regarding the commutator of the density operators. The key point in this model is the recognition that the low-energy excitations of the 1D electron gas are electron-hole pairs which are approximate bosons, though the elementary particles are fermions. Since the excitations involve two-fermion states, the wave function will have the bosonic properties. And the bosonization technique allows us to solve the interacting problem and to extract a certain number of properties such as power law behavior of the correlation functions.

Later, Luttinger proposed a better model [1] for spinless 1D interacting fermions introducing some new states and this model is also exactly soluble. The model shows certain extraordinary properties viz. there is no low-energy fermionic quasiparticle in the system, the usual definition of the Fermi surface fails and the correlation functions decay asymptotically at large distance. The 1D Hubbard model and the 1D XXZ model also behave in the same way. The concept of LL encompasses most of the physics of simple 1D systems and is the starting point to study more complex situations.

2.1.1 Dispersion relation

The basic feature of the Luttinger model is that the system has two types of fermions which obey the linear dispersion relation as follows:

$$\text{Type - 1: } \epsilon_k = kv_F \qquad \text{and} \qquad \text{type - 2: } \epsilon_k = -kv_F \qquad (2.1)$$

and the two energy bands are independent. The ground state of the Luttinger model was not bounded from below and Lieb and Mattis [6] rectified this error and again solved the problem exactly. Luther and Peschel [7] calculated the electron spectral density, susceptibility and pair propagation of an interacting electron system within the framework of the Luttinger model. Haldane [8] used the Luttinger model for the description of the general interacting Fermi gas in one-dimension and called it a LL. Yoshioka and Ogata [9] obtained the asymptotically exact ground state for 1D electrons and studied the transition from a LL behaviour to a non-Luttinger liquid behaviour as a function of some parameter which appears in the electron-electron interaction coefficient.

Photoluminescence experiments from real quantum wires show the existence of a sharp Fermi surface [10]. Hu and Das [11] suggested that virtual plasmon emissions that are present in systems would be inhibited in dirty systems leading to the restoration of the Fermi surface. Adding to the Luttinger Hamiltonian a parametrized term that accounts for the scattering of plasmons by the impurities existing in real systems, Melgarejo and Vericat [12] showed that Fermi surface was indeed restored in the presence of the impurities. Wonneberger [13] have investigated the density and the electron distribution function of a LL confined to a harmonic trap. Wang et al. [14] presented accurate expressions for the effect of the long-range

electron-electron interaction on momentum distribution, density of states, electron spectral function etc. of a 1D LL. Schönhammer [15] also obtained the momentum distribution function of electrons and the spectral function of a LL. Sen and Chakrabarti [16] employed density functional theory to establish the LL behavior of a sodium-doped quasi-one-dimensional trans-polyacetylene chain. Many theoretical works have been done on carbon nonotubes to understand the effects of the electron-electron interactions using the celebrated Luttinger-liquid theory [17].

All these investigations, however, neglected the lattice excitations like phonons and their interactions with electrons, which actually play an important role in the transport phenomena and are relevant in polar semiconductors. Also the experimental observation of superconductivity in ropes of nanotubes has motivated theoretical studies of the electron-phonon interactions. Several investigations [18] were however made on 1D many-polaron problem using the quadratic electron dispersion. It is been shown that with the reduction in the dimensionality of the systems, the effects of electron-phonon interactions become more predominant. Baldea [19] was probably the first to study an interacting electron system including phonons using the linear electron dispersion. He considered the interaction of electrons with long-wavelength acoustic-phonons within the framework of Tomonaga model and calculated the momentum distribution function. Marino [20] considered a 1D acoustic many-polaron Hamiltonian within the framework of the Luttinger model and showed that for a certain range of the coupling constants the system would exhibit a metallic behavior since the spectrum contains gapless collective excitations of polaronic plasmons. Later, Martins [21] considered a problem with both electron-optical-phonon

interaction and the electron-acoustic-phonon interaction but neglected the electron-electron interaction.

Recently, Rao et al. [22] have exactly solved the 1D interacting electron problem within the framework of Luttinger model incorporating both the electron-optical-phonon interaction and the electron-acoustic-phonon interaction along with the electron-electron interaction, to obtain the energy spectrum. This system can be referred to as the Fröhlich-Toyozawa-Luttinger (FTL) liquid. It seems that metallicity of the system depends crucially on the nature of the electron-electron interaction in one-dimension. To our knowledge, however, no investigation has so far been made to obtain the momentum distribution function of electrons in a LL in the presence of the electron-phonon interactions. So, in this chapter our aim is to make an attempt in this direction.

2.2 Theoretical Formalism and calculation of energy

The total Hamiltonian for the fully interacting 1D electron can be written as

$$H = H_{el} + H_{ph}^{op} + H_{ph}^{ac} + H_{ep}^{op} + H_{ep}^{ac} + H_{el-el} \tag{2.1}$$

where, H_{el} is the free electron Hamiltonian, H_{ph}^{op} is the free optical-phonon Hamiltonian, H_{ph}^{ac} is the free acoustic-phonon Hamiltonian, H_{ep}^{op} is the electron-optical-phonon interaction term, H_{ep}^{ac} is the electron-acoustic-phonon interaction term and H_{el-el} is the electron-electron

interaction term. Let us look into each term carefully. The free-electron Hamiltonian is,

$$H_{el} = \sum_k k\hbar v_F \left(a_{1k}^\dagger a_{1k} - a_{2k}^\dagger a_{2k}\right) \tag{2.2}$$

where v_F is the Fermi velocity, $a_{1k}^\dagger(a_{1k})$ and $a_{2k}^\dagger(a_{2k})$ are the creation (annihilation) operators for the type-1 and type-2 fermions respectively and they satisfy the canonical anti-commutation relations, $\left\{a_{i,k}\,,\, a_{j,k'}^\dagger\right\} = \delta_{ij}\delta_{kk'}, i,j = 1,2$. The optical-phonon Hamiltonian is,

$$H_{ph}^{op} = \sum_k \hbar\omega_0 b_k^\dagger b_k \ , \tag{2.3}$$

where, $b_k^\dagger\ (b_k)$ is the creation (annihilation) operator for an optical-phonon of frequency ω_0. The acoustic-phonon Hamiltonian is,

$$H_{ph}^{ac} = \sum_k \hbar v_s |k| \tilde{b}_k^\dagger \tilde{b}_k \ , \tag{2.4}$$

where, v_s is the velocity of sound and $\tilde{b}_k^\dagger(\tilde{b}_k)$ is the creation (annihilation) operator for an acoustic-phonon. Degani et al. [23] have used the Feynman path integral formalism to calculate the energy and the effective mass of 1D optical and acoustic polarons. They have observed that the optical-polarons yield a continuous change as the interaction strength goes from weak to strong limit while the acoustic-polaron state shows an abrupt change for certain value of the coupling constant. Keeping these points in mind we can write the Hamiltonian for electron-optical-phonon interaction as

$$H_{ep}^{op} = \frac{g^{'}}{\sqrt{2L}} \sum_{k} \sqrt{\hbar\omega_0}\,[\rho_1(k) + \rho_2(k)]\left(b_k + b_{-k}^{\dagger}\right), \qquad (2.5)$$

with $g^{'} = \sqrt{8\pi\hbar g} \times (\hbar\omega_0/2m)^{1/4}$, g being the dimensionless electron-optical-phonon coupling constant, L is the length of the system and $\rho_i(k)$ is the electron density operator and is given by

$$\rho_i(k) = \sum_{q} a_{i,q+k}^{\dagger} a_{i,q}\ , \quad i = 1,2. \qquad (2.6)$$

The Hamiltonian for electron-acoustic-phonon interaction is given by

$$H_{ep}^{ac} = i\frac{\lambda^{'}}{\sqrt{2L}} \sum_{k>0} \sqrt{\hbar v_s|k|}\,[\rho_1(k) + \rho_2(k)]\left(\tilde{b}_k + \tilde{b}_{-k}^{\dagger}\right) + H.C, \qquad (2.7)$$

with $\lambda^{'} = -i\sqrt{8\pi\hbar v_s\lambda}$, λ being the dimensionless electron-acoustic-phonon coupling constant. Now, let us write the electron-electron Hamiltonian as

$$H_{el-el} = \frac{1}{2}\int \psi^{\dagger}(x)\psi^{\dagger}(y)\, V(|x-y|)\psi(y)\psi(x)\, dxdy\,, \qquad (2.8)$$

where $V(|x-y|)$ represents the electron-electron interaction potential which is a function of $|x-y|$ and $\psi(x)$ is the two-component field operator given by $\psi = \begin{pmatrix} \psi_1(x) \\ \psi_2(x) \end{pmatrix}$, where,

$$\psi_i(x) = \frac{1}{\sqrt{L}} \sum_{k} e^{ikx}\, a_{ik} \qquad (2.9)$$

Now we write the total Hamiltonian in terms of these field operators as

$$H = -i\hbar v_F \int \psi^\dagger(x)\sigma_3\,\partial_x\psi(x)dx + \frac{1}{2}\int\left[\dot{\phi}^2(x) + \hbar^2\omega_0^2\phi^2(x)\right]dx$$
$$+ \frac{1}{2}\int\left[\dot{\tilde{\phi}}^2(x) + \hbar^2 v_s^2\left(\partial_x\tilde{\phi}(x)\right)^2\right]dx + g'\hbar\omega_0\int\psi^\dagger(x)\,\psi(x)\phi(x)dx$$
$$+ \lambda'\hbar v_s\int\psi^\dagger(x)\psi(x)\partial_x\tilde{\phi}(x)dx$$
$$+ \frac{1}{2}\iint\psi^\dagger(x)\psi^\dagger(y)\,V(|x-y|)\,\psi(y)\psi(x)\,dxdy\,, \qquad (2.10)$$

where σ_3 is the Pauli matrix,

$$\phi(x) = \sum_k \frac{1}{\sqrt{2L\hbar\omega_0}}\left(b_k + b_{-k}^\dagger\right)e^{ikx}$$

is the optical-phonon field operator and

$$\tilde{\phi}(x) = \sum_k \frac{1}{\sqrt{2L\hbar v_s|k|}}\left(\tilde{b}_k + \tilde{b}_{-k}^\dagger\right)e^{ikx}$$

is the acoustic-phonon field operator.

We have to eliminate both optical and acoustic phonon fields to describe the dynamics of the system in terms of polaron. In order to accomplish that we introduce the Lagrangian density corresponding to the Hamiltonian, $\mathcal{H}$ as

$$\mathcal{L} = i\psi^\dagger(x)\partial_t\psi(x) + i\hbar v_F\psi^\dagger(x)\sigma_3\partial_x\psi(x) + \frac{1}{2}[\dot{\phi}^2(x) - \hbar^2\omega_0^2\phi^2(x)]$$
$$- g'\hbar\omega_0\,\psi^\dagger(x)\psi(x)\phi(x) - \lambda'\hbar v_s\psi^\dagger(x)\psi(x)\partial_x\tilde{\phi}(x) + \dot{\phi}\chi + \dot{\tilde{\phi}}\,\tilde{\chi}$$
$$+ \frac{1}{2}[\dot{\tilde{\phi}}^2(x) - \hbar^2 v_s^2\left(\partial_x\tilde{\phi}(x)\right)^2]$$

$$-\frac{1}{2}\iint \psi^{\dagger}(x)\psi^{\dagger}(y)V|x-y|\psi(y)\psi(x)\,dxdy\,, \tag{2.11}$$

where $\dot{\phi}\chi$ and $\dot{\tilde{\phi}}\,\tilde{\chi}$ are the two additional terms we have introduced which will not affect the Lagrangian equation of motion and Hamiltonian density. And now we need to choose χ and $\tilde{\chi}$ in such a way that we can eliminate the phonon fields from the problem. In Lagrange's equations of motion we will take,

$$\chi = -\dot{\phi} \quad \text{and} \quad \tilde{\chi} = -\dot{\tilde{\phi}}\,,$$

which yields

$$\varphi(x) = -\frac{g}{\omega_0}\psi^{\dagger}(x)\psi(x) \quad \text{and} \quad \partial_x\tilde{\phi}(x) = -\frac{\lambda}{v_s}\psi^{\dagger}(x)\psi(x)\,, \tag{2.12}$$

To proceed further we perform the following transformations,

$$\psi(x) \rightarrow \psi'(x) = e^{i\theta}\,\psi(x),$$

and

$$\psi(x) \rightarrow \psi'(x) = e^{i\sigma_3\theta}\,\psi(x),$$

under which the Lagrangian density remains invariant and we get two conservation laws. These conservation equations along with the Lagrange's equations of motion show that the two phonon fields are decoupled.

With this knowledge we can write the Hamiltonian as

$$H = -i\hbar v_F \int \psi^{\dagger}(x)\sigma_3\,\partial_x\psi(x)dx + \frac{1}{2}\frac{g'v_F^2}{\omega_0^2}\int\left(\frac{\partial}{\partial x}\psi^{\dagger}(x)\sigma_3\psi(x)\right)^2 dx$$

$$-\frac{1}{2}\left(g'^{2}+\lambda'^{2}\right)\int\left(\psi^{\dagger}(x)\psi(x)\right)^{2}dx$$

$$+\frac{1}{2}\iint\psi^{\dagger}(x)\psi^{\dagger}(y)V|x-y|\psi(y)\psi(x)\,dxdy$$

$$+\frac{1}{2}\frac{\lambda'^{2}v_F^2}{v_s^2}\int\left(\psi^{\dagger}(x)\sigma_3\psi(x)\right)^{2}dx\ . \tag{2.13}$$

We can write

$$\psi^{\dagger}(x)\sigma_3\partial_x\psi(x)=\frac{1}{L}\sum_{kk'}ike^{i(k-k')x}\left(a_{1k'}^{\dagger}a_{1k}-a_{2k'}^{\dagger}a_{2k}\right), \tag{2.14}$$

$$\frac{\partial}{\partial x}\psi^{\dagger}(x)\sigma_3\psi(x)=\frac{1}{L}\sum_{k}ike^{ikx}\left[\rho_1(-k)-\rho_2(-k)\right], \tag{2.15}$$

$$\psi_i^{\dagger}(x)\psi_i(x)=\frac{1}{L}\sum_{k}\rho_i(-k)e^{ikx}\ , \tag{2.16}$$

$$\psi_i^{\dagger}(x)\sigma_3\psi_i(x)=\frac{1}{L}\sum_{k}e^{ikx}[\rho_1(-k)-\rho_2(-k)]\ . \tag{2.17}$$

The electron-electron Hamiltonian can be rewritten using the density operators as

$$H_{el-el}=\frac{1}{2L}\sum_{k>0}V_{1k}\left[\rho_1(k)\rho_1(-k)+\rho_2(-k)\rho_2(k)\right]$$
$$+\frac{1}{2L}\sum_{all\ k}V_{1k}\ \rho_1(k)\rho_2(-k)\,, \tag{2.18}$$

where,

$$V_{1k}=V_k+V_{-k},$$

and V_k is the Fourier transform of $V(|x-y|)$

$$V_k = \iint V|x-y|e^{iq(x-y)}dxdy \tag{2.19}$$

It may be noted that our calculation includes the Coulomb interaction between the two types of electrons too. Now, with all these results the Hamiltonian can be written as

$$\begin{aligned} H &= H_{el} + H_{el-el}^{eff} \\ &= \sum_k k\hbar v_F\left(a_{1k}^{\dagger}a_{1k} - a_{2k}^{\dagger}a_{2k}\right) \\ &+ \sum_{k>0}\left[\frac{1}{2L}\left\{2g_{\perp 2}\left(\frac{v_F^2k^2}{\omega_0^2}-1\right)\right\} + \frac{\lambda_{\perp 2}}{L}\left(\frac{v_F^2}{v_s^2}-1\right) + \frac{V_{1k}}{2L}\right] \\ &\qquad \times [\rho_1(k)\rho_1(-k) + \rho_2(-k)\rho_2(k)] \\ &- \sum_{all\ k}\left[\frac{1}{2L}\left\{2g_{\perp 2}\left(\frac{v_F^2k^2}{\omega_0^2}+1\right)\right\} + \frac{\lambda_{\perp 2}}{L}\left(\frac{v_F^2}{v_s^2}+1\right) - \frac{V_{1k}}{2L}\right]\rho_1(k)\rho_2(-k). \end{aligned} \tag{2.20}$$

For further simplifications, we use the commutation relations of the density operator $\rho_i(k)$ which are bosonic in nature

$$\left[\rho_i(-k), \rho_j(k')\right] = (-1)^{i+1}\,\delta_{ij}\,\delta_{kk'}\left(\frac{kL}{2\pi}\right) \quad (\text{with } k, k' > 0\ ,\ \ i,j = 1,2) \tag{2.21}$$

and then we replace the free-electron Hamiltonian H_{el} by an operator T given by

$$T = \frac{2\pi}{L}v_F\sum_{k>0}[\rho_1(k)\rho_1(-k) + \rho_2(-k)\rho_2(k)]\ , \tag{2.22}$$

which has the same commutation relations with ρ as H_{el}. So we could write the Hamiltonian as

$$H = \sum_{k>0}\left[\frac{1}{2L}\left\{2g'^{2}\left(\frac{v_F^2k^2}{\omega_0^2}-1\right)+4\pi\hbar v_F\right\}+\frac{\lambda'^{2}}{L}\left(\frac{v_F^2}{v_s^2}-1\right)+\frac{V_{1k}}{2L}\right] \times [\rho_1(k)\rho_1(-k)+\rho_2(-k)\rho_2(k)]$$

$$+\sum_{all\ k}\left[-\frac{1}{2L}\left\{2g'^{2}\left(\frac{v_F^2k^2}{\omega_0^2}+1\right)\right\}-\frac{\lambda'^{2}}{L}\left(\frac{v_F^2}{v_s^2}+1\right)+\frac{V_{1k}}{2L}\right]\rho_1(k)\rho_2(-k). \quad (2.23)$$

Now, the above Hamiltonian can be diagonalized by the unitary transformation using the generator,

$$S = \frac{2\pi i}{L}\sum_{all\ k}\frac{\phi(k)}{k}\rho_1(k)\rho_2(-k)\ , \quad (2.24)$$

where $\phi(k)$ is a real and even function of k and the conditions for diagonalization gives,

$$\phi(k) = \frac{1}{2}tanh^{-1}\left(-\frac{D_2(k)}{D_1(k)}\right)\ , \quad (2.25)$$

with

$$D_1(k) = \frac{1}{2L}\left[\left\{2g'^{2}\left(\frac{v_F^2k^2}{\omega_0^2}-1\right)+4\pi\hbar v_F\right\}+2\lambda'^{2}\left(\frac{v_F^2}{v_s^2}-1\right)+V_{1k}\right] \quad (2.26)$$

and

$$D_2(k) = \frac{1}{2L}\left[-\left\{2g'^{2}\left(\frac{v_F^2k^2}{\omega_0^2}+1\right)\right\}-2\lambda'^{2}\left(\frac{v_F^2}{v_s^2}+1\right)+V_{1k}\right] \quad (2.27)$$

2.2.1 The energy spectrum

After the unitary transformation the Hamiltonian can mapped on to a Harmonic oscillator and the energy spectrum can be obtained as

$$\epsilon(k) = \hbar v_F |k| \left(1 - \frac{g'^2 + \lambda'^2}{\pi\hbar v_F} + \frac{V_{1k}}{2\pi\hbar v_F}\right)^{1/2} \times \left(1 + \frac{g'^2 k^2 v_F}{\pi\hbar\omega_0^2} + \frac{\lambda'^2 v_F}{\pi\hbar v_s^2}\right)^{1/2}. \quad (2.28)$$

From the energy expression it is very clear that the whole calculation is valid only if the coupling parameters satisfy the following condition:

$$g_c'^2 + \lambda_c'^2 < \left(\pi\hbar v_F + \frac{V_{1k}}{2}\right). \quad (2.29)$$

From Eqn. (2.28) it is clear that for a certain range of coupling constant the energy spectrum of the system is gapless and we would then have a polaronic metal. To plot the energy spectrum $\epsilon(k)$ we need an explicit form for V_{1k}. We choose the form of the potential by following Wang et al. [14] as

$$V_{1k} = 4\pi\mu e^2 \ln(1 + k_F/k) \quad (2.30)$$

where μ is the electron-electron coupling constant.

In Fig. 2.1 we plot the dimensionless excitation energy $\epsilon(k)$ (in units of Rydberg), for various interactions. We define the effective electron-optical-phonon coupling constant as $\alpha_{op} = (4\pi g\omega_0'^{3/2}/L')^{1/2}$ and the effective electron-acoustic-phonon coupling constant as $\alpha_{ac} = (16\pi\lambda v_s'^2/L')^{1/2}$,

where the primed quantities are dimensionless in Rydberg units. As expected, the electron-electron interaction increases the energy, while the polaron formation decreases it.

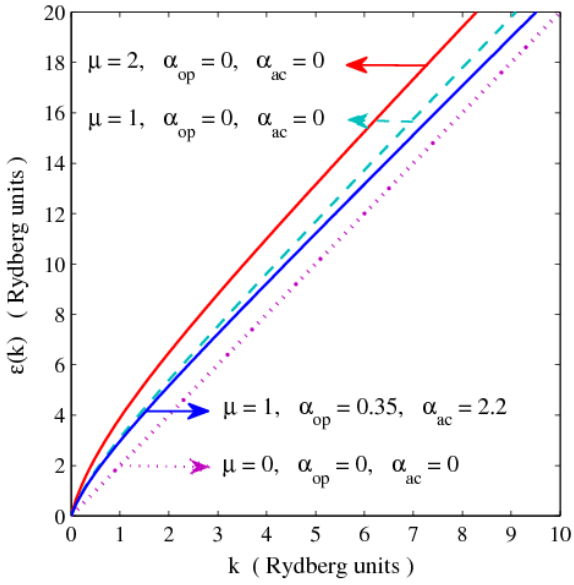

Fig. 2.1 Energy spectrum of a Luttinger liquid for various interactions and interaction strengths.

2.3 Evaluation of the Momentum Distribution Function

Here we calculate for the first time the electron distribution function $\bar{n}_k$, for the FTL liquid. This calculation is important since most of the interesting applications of the Luttinger model are concerned with the single-particle properties of the interacting electron system. The momentum distribution function $\bar{n}_k$ is an even function of k, hence we need to consider only $k > 0$ and it will also suffice to calculate $\bar{n}_k$ only for particle

type-1. We know that $a_{1k}^{\dagger}$ (a_{1k}) is the creation (annihilation) operators for the type-1 fermions and for $k > 0$ we have defined $a_{1k} = c_k$.

$$\bar{n}_k = \langle a_{1k}^{\dagger} a_{1k} \rangle = \langle c_k^{\dagger} c_k \rangle \tag{2.31}$$

where $c_k^{\dagger}$ (c_k) for $k > 0$ creates (destroys) a particle of type-1 with positive energy. From Eqn. (2.9) we know that $c_k^{\dagger}$, c_k are related to the field operator ψ ′s through Fourier transformations

$$c_k^{\dagger} = \frac{1}{\sqrt{L}} \int \psi_1^{\dagger}(x) e^{ikx} dx \,, \tag{2.32}$$

and

$$c_k = \frac{1}{\sqrt{L}} \int \psi_1(x) e^{-ikx} dx \,. \tag{2.33}$$

Then

$$\bar{n}_k = \frac{1}{L} \iint_0^L I(x, x') \, e^{ik(x-x')} dx dx' \,, \tag{2.34}$$

where

$$I(x, x') = \langle \Psi | \psi_1^{\dagger}(x) \psi_1(x') | \Psi \rangle \tag{2.35}$$

is the correlation function, $|\Psi\rangle$ being the ground state of the interacting system. Using the transformations: $e^{iS} H e^{-iS} = \tilde{H}$ and $e^{iS} |\Psi\rangle = |\Psi_0\rangle$, the Hamiltonian becomes diagonal and we can write the correlation function as

$$I(x, x') = \langle \Psi_0 | e^{iS} \psi_1^{\dagger}(x) e^{-iS} e^{iS} \psi_1(x') e^{-iS} | \Psi_0 \rangle \tag{2.36}$$

where $|\Psi_0\rangle$ is the new ground state of the non-interacting system. To calculate the correlation function we introduce as usual an auxiliary operator

$$f_\sigma(x) = e^{i\sigma S}\psi_1(x)e^{-i\sigma S} \tag{2.37}$$

so that $f_0(x) = \psi_1(x)$ and $f_1(x) = e^{iS}\psi_1(x)e^{-iS}$. Also

$$\frac{\partial f}{\partial \sigma} = e^{i\sigma S}\left[\frac{2\pi}{L}\sum_k \frac{\phi(k)}{k}\rho_2(-k)e^{ikx}\right]e^{-i\sigma S}f_\sigma(x)\,. \tag{2.38}$$

By solving the above differential equation we get,

$$f_\sigma(x) = W_\sigma(x)R_\sigma(x)\psi_1(x)\,, \tag{2.39}$$

where

$$W_\sigma(x) = exp\left\{\sum_{k>0}\left(\frac{2\pi}{kL}\right)\eta_1(k,x)(cosh\sigma\phi(k)-1)\right\}, \tag{2.40}$$

$$R_\sigma(x) = exp\left\{\sum_{k>0}\left(\frac{2\pi}{kL}\right)\eta_2(k,x)sinh\sigma\phi(k)\right\}\,, \tag{2.41}$$

and

$$\psi_1(x) = c(x)exp\left\{\sum_{k>0}\left(\frac{2\pi}{kL}\right)\eta_1(k,x)\right\}, \tag{2.42}$$

with

$$\eta_i(k,x) = \left[\rho_i(-k)e^{ikx} - \rho_i(k)e^{-ikx}\right]\,. \tag{2.43}$$

Now we will set $\sigma = 1$ and call $W_1(x) = W(x)$ and $R_1(x) = R(x)$. Then

$$f_1(x) = W(x)R(x)\psi_1(x)\,. \tag{2.44}$$

Thus the correlation function becomes

$$I(x,x') = \langle\Psi_0|\psi_1^\dagger(x)R^\dagger(x)W^\dagger(x)W(x')R(x')\,\psi_1(x')|\Psi_0\rangle\,. \tag{2.45}$$

Since $\rho_1^\dagger(k) = \rho_1(-k)$ and $\rho_2^\dagger(k) = \rho_2(-k)$, we can immediately show that $R(x)$ and $W(x)$ are unitary and also they commute with each other. Since there are two types of electrons in our system, the ground state is a product state,

$$|\Psi_0\rangle = |\Psi_1\rangle\,|\Psi_2\rangle\,. \tag{2.46}$$

Now we can write Eqn. (2.45) as

$$I(x,x') = I_1(x,x')I_2(x,x')\,, \tag{2.47}$$

where

$$I_1(x,x') = \langle\Psi_1|\psi_1^\dagger(x)W^{-1}(x)W(x')\psi_1(x')|\Psi_1\rangle\,, \tag{2.48}$$

and

$$I_2(x,x') = \langle\Psi_2|R^{-1}(x)R(x')|\Psi_2\rangle\,. \tag{2.49}$$

Using the Becker-Hausdroff identity

$$e^A\,e^B = e^{A+B}\,e^{\frac{1}{2}[A,B]}\,, \tag{2.50}$$

and the properties of $\rho(k)$ we can show that,

$$W^{-1}(x)W(x') = W_-(x,x')W_+(x,x')Z_1(x,x')\,, \tag{2.51}$$

where

$$W_{-}(x,x') = \exp\left\{\frac{2\pi}{L}\sum_{k>0}\rho_1(k)\left[\frac{cosh\phi(k)-1}{k}\right]\left(e^{-ikx}-e^{-ikx'}\right)\right\}, \quad (2.52)$$

$$W_{+}(x,x') = \exp\left\{\frac{2\pi}{L}\sum_{k>0}\rho_1(-k)\left[\frac{cosh\phi(k)-1}{k}\right]\left(e^{ikx'}-e^{ikx}\right)\right\}, \quad (2.53)$$

and

$$Z_1(x,x') = exp\left\{\frac{2\pi}{L}\sum_{k>0}\frac{(cosh\phi(k)-1)^2}{k}\left(e^{ik(x-x')}-1\right)\right\}. \quad (2.54)$$

Similarly,

$$R^{-1}(x)R(x') = R_{-}(x,x')R_{+}(x,x')Z_2(x,x') \quad (2.55)$$

where

$$R_{-}(x,x') = \exp\left\{\frac{2\pi}{L}\sum_{k>0}\rho_2(-k)\left[\frac{sinh\phi(k)}{k}\right]\left(e^{ikx'}-e^{ikx}\right)\right\}, \quad (2.56)$$

$$R_{+}(x,x') = \exp\left\{\frac{2\pi}{L}\sum_{k>0}\rho_2(k)\left[\frac{sinh\phi(k)}{k}\right]\left(e^{-ikx}-e^{-ikx'}\right)\right\}, \quad (2.57)$$

and

$$Z_2(x,x') = exp\left\{\frac{2\pi}{L}\sum_{k>0}\frac{[sinh\phi(k)]^2}{k}\left(e^{ik(x'-x)}-1\right)\right\}. \quad (2.58)$$

From the definition of the density operators, it is very clear that for $k > 0$,

$$\rho_1(-k)|\Psi_1\rangle = 0 \quad \text{and} \quad \langle\Psi_1|\rho_1(k) = 0\,, \quad (2.59)$$

$$\rho_2(k)|\Psi_2\rangle = 0 \quad \text{and} \quad \langle\Psi_2|\rho_2(-k) = 0\,. \quad (2.60)$$

This will lead us to write

$$I_2(x,x') = Z_2(x,x')\,. \tag{2.61}$$

Using Eqn. (2.51) we can write

$$I_1(x,x') = Z_1(x,x')\langle\Psi_1\left|\psi_1^{\dagger}(x)W_-(x,x')W_+(x,x')\psi_1(x')\right|\Psi_1\rangle\,. \tag{2.62}$$

Also, we can show that

$$W_+^{-1}(x,x')|\Psi_1\rangle = |\Psi_1\rangle \quad \text{and} \quad \langle\Psi_1|W_-^{-1}(x,x') = |\Psi_1\rangle\,. \tag{2.63}$$

With this the above equation can be written as

$$I_1(x,x') = Z_1(x,x')\langle\Psi_1\left|W_-^{-1}(x,x')\psi_1^{\dagger}(x)W_-(x,x')W_+(x,x')\psi_1(x')W_+^{-1}(x,x')\right|\Psi_1\rangle \tag{2.64}$$

Now we will define,

$$h_+(y) = \frac{2\pi}{L}\sum_{k>0}\left[\frac{cosh\phi(k)-1}{k}\right]\left(e^{ikx'}-e^{ikx}\right)e^{-iky}\,, \tag{2.65}$$

$$h_-(y) = \frac{2\pi}{L}\sum_{k>0}\left[\frac{cosh\phi(k)-1}{k}\right]\left(e^{-ikx'}-e^{-ikx}\right)e^{iky}\,. \tag{2.66}$$

Combining the above equations with $\rho_1(y) = \frac{1}{L}\sum_{all\,k}\rho_1(-k)e^{iky}$, we can get

$$W_-(x,x') = exp\left\{-\int_0^L \rho_1(y)h_-(y)dy\right\}\,, \tag{2.67}$$

and

$$W_+(x,x') = exp\left\{\int_0^L \rho_1(y)h_+(y)dy\right\}\ , \tag{2.68}$$

Also, we have

$[\psi_1(x),\rho_1(y)] = \delta(x-y)\psi_1(y)$ and

$$\left[\psi_1^\dagger(x),\rho_1(y)\right] = -\delta(x-y)\psi_1^\dagger(y). \tag{2.69}$$

With these equations and using the identity

$$e^S A e^{-S} = A + [S,A] + \frac{1}{2!}\big[S,[S,A]\big] + \cdots \tag{2.70}$$

we can find that

$$W_-^{-1}(x,x')\psi_1^\dagger(x)W_-(x,x') = \psi_1^\dagger(x)exp\{h_-(x)\}\,, \tag{2.71}$$

and

$$W_+(x,x')\psi_1\,(x')W_+^{-1}(x,x') = \psi_1(x')exp\{-h_+(x')\}\,. \tag{2.72}$$

Finally, the correlation function can be written as

$$I(x,x') = Z_0(x,x')Z_1(x,x')Z_2(x,x')Z_3(x,x') \tag{2.73}$$

where

$$Z_0(x,x') = exp\left\{\frac{-4\pi}{L}\sum_{k>0}\left(\frac{cosh\phi(k)-1}{k}\right)\left[1-e^{ik(x-x')}\right]\right\} \tag{2.74}$$

and

$$Z_3(x,x') = \langle\Psi_1\big|\psi_1^\dagger(x)\psi_1(x')\big|\Psi_1\rangle = \frac{1}{L}\sum_{p\le k_F} e^{ip(x'-x)} \tag{2.75}$$

where $Z_1(x,x')$ and $Z_2(x,x')$ have already been defined above. All these Z_i's above are functions of $(x-x')$. Put $(x-x')=r$ and define a function $Q(r)$ as

$$e^{-Q(r)} = Z_0(r)Z_1(r)Z_2(r) \ . \tag{2.76}$$

Then the distribution function can be written as

$$\bar{n}_k = \frac{1}{L}\sum_{p\le k_F}\int_{-L}^{L} dr\ e^{i(k-p)r}\ e^{-Q(r)} \ . \tag{2.77}$$

Substituting the values of Z_i's we can get,

$$Q(r) = \int_0^{\infty} \frac{(1-coskr)}{k}\ 2sinh^2\phi(k)\,dk \ . \tag{2.78}$$

In the previous section we have gotten $tanh2\,\phi(k) = -\frac{D_2(k)}{D_1(k)}$ and this result will help us to write $2sinh^2\phi(k)$ which will be denoted as $|u(k)|^2$, so that the expression for $Q(r)$ will look similar to that of Lieb-Mattis and Luttinger.

So let us write

$$Q(r) = \int_0^{\infty} \frac{(1-coskr)}{k}(|u(k)|^2)\,dk \ , \tag{2.79}$$

where

$$|u(k)|^2 = \left[\frac{D_1(k)-\sqrt{D_1^2(k)-D_2^2(k)}}{\sqrt{D_1^2(k)-D_2^2(k)}}\right]. \tag{2.80}$$

Now take the bulk limit $L \to \infty$ and define

$$F(k) = \left(\frac{1}{2\pi}\right) \int_{-\infty}^{\infty} dr\, e^{-Q(r)}\, e^{ikr} \,. \tag{2.81}$$

Then the distribution function will take up the following form

$$\bar{n}_k = \frac{2\pi}{L} \sum_{p \le k_F} F(k-p) \,. \tag{2.82}$$

Now by changing the summation to integration and by putting $(k-p) = k^{"}$, we can write

$$\bar{n}_k = \int_{k-k_F}^{0} F(k^{"}) dk^{"} + d \,. \tag{2.83}$$

where d is a constant. The above expression for $\bar{n}_k$ is similar to that of Lieb-Mattis, except for the fact that $|u(k)|^2$ which contains the interactions is different. Lieb-Mattis contains only one type of electron-electron interaction while we have considered two types of electron-electron interactions and the interaction between these two types of electrons along with the electron-phonon interaction terms. It can be easily shown that when there is no interaction we get the usual Fermi-Dirac distribution with a sharp Fermi surface.

To check whether a sharp Fermi surface exists even when we include interactions, we have done the following calculation. First of all we have turned off the electron-phonon interactions and included only the electron-electron interaction V_{1k} which we kept as a constant so that in co-ordinate

space it is a δ- function interaction, then after some algebraic exercise we could get an expression for $e^{-Q(r)}$ as:

$$e^{-Q(r)} = \lim_{\alpha \to 0} \frac{1}{\left(1 + \frac{r^2}{\alpha^2}\right)^{A/2}} \quad , \tag{2.84}$$

where A contains the electron-electron interaction and is a constant. Substitute for $e^{-Q(r)}$ in $\bar{n}_k$ and then set $A = 0$, which will be the case when there is no interaction and we get,

$$\bar{n}_k = \int_{-\infty}^{k_F} \delta(k - p) dp \tag{2.85}$$

which shows the existence of a sharp Fermi surface.

Now, to check the case when $A \to 0$ we had to perform a change the variable: $r/\alpha = y$ and then by putting $y = tan\theta$ we get,

$$\bar{n}_k = \frac{1}{2\pi^{\frac{1}{2}}} \quad \frac{\Gamma\left(\frac{A}{2} + \frac{1}{2}\right)}{\Gamma\left(1 + \frac{A}{2}\right)} \, . \tag{2.86}$$

In the limit $A \to 0$, the distribution function $\bar{n}_k = 1/2$. So, for $A = 0$ and $A \to 0$ the results are not at all the same, which indicates that the Fermi surface may break down.

Lieb and Mattis have shown that near the Fermi surface, with proper assumption of the electron-electron interaction term, the distribution function behaves like,

$$\bar{n}_k = d - e|k - k_F|^{2D}\sigma(k - k_F) \ , \tag{2.87}$$

where

$$\sigma(k - k_F) = \begin{cases} 1, & k > k_F \\ -1, & k < k_F \end{cases} \ , \tag{2.88}$$

with *d*, *e* and *D* being positive constants given by

$$d = \int_0^\infty F(k)dk \ , \quad e = \frac{a^{2D}}{2D\pi}\Gamma(1 - 2D)sin(\pi D) \quad \text{and} \quad D = \frac{1}{2}(|u(0)|^2).$$

Lieb and Mattis have concluded that for $2D < 1$, the interactions removes the discontinuity but, still there exists a residual Fermi surface at $k = k_F$ since $lim_{k \to k_F} \frac{d\bar{n}_k}{dk}$ diverges. But for $2D > 1$, there is no infinite slope and $\bar{n}_k$ is a smooth function. Hence they have concluded that a strong Coulomb interaction would destroy the Fermi surface completely. In our calculation, to get the Lieb-Mattis expression for $\bar{n}_k$, we have to take $V_{1k} = 1/k^2$. But the form: $1/k^2$ does not give the proper description of the excitation spectrum. So we choose the form which is discussed earlier in Eqn. (2.30).

Here, we wish to study how $\bar{n}_k$ [Eqn. (2.83)] is particularly modified by the electron-phonon interactions. Using the expressions for $|u(k)|^2$ [Eqn. (2.80)] , $Q(r)$ [Eqn. (2.79)] and $F(k)$ [Eqn. (2.81)] , we can obtain the exact momentum distribution function $\bar{n}_k$ numerically. Again we choose for V_{1k} the prescription of Wang et al. [13].

2.4 Numerical Results

In Fig. 2.2 we plot $\bar{n}_k$ for several values of μ with $\alpha_{op} = \alpha_{ac} = 0$. For $\mu = 0$, the usual Fermi-Dirac distribution with a sharp Fermi surface is clearly visible. And as μ increases the Fermi surface begins to disappear.

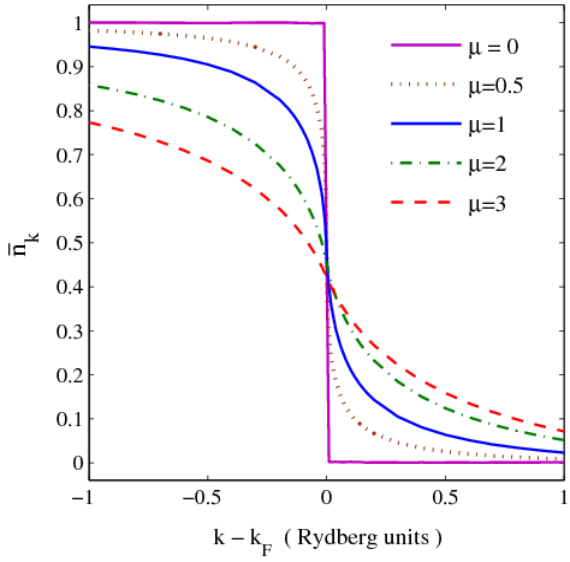

Fig. 2.2 Momentum distribution function of electrons in a Luttinger liquid for various values of the electron-electron interaction coefficient.

Wang et al. [13] have studied the behavior of $(0.5 - \bar{n}_k)$ vs. $(k - k_F)$ for $k \geq k_F$. To compare our results qualitatively with theirs we plot $(0.5 - \bar{n}_k)$ in Fig. 2.3. Our results clearly show the same behavior as those of Wang et al.

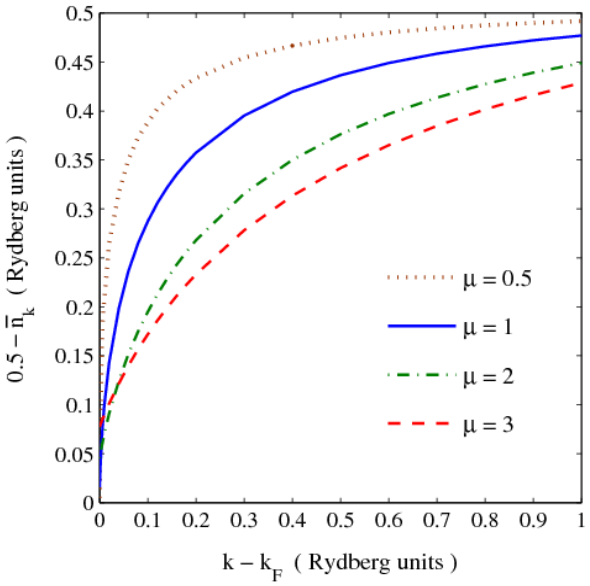

Fig. 2.3 Variation of $(0.5 - \bar{n}_k)$ as a function of $(k - k_F)$.

In Fig. 2.4 we plot the derivative of the momentum distribution function i.e., $[-(d\bar{n}_k/dk)]$ as a function of k. It is evident from the behavior of $[-(d\bar{n}_k/dk)]$ that for $\mu = 1$, the distribution function has a singularity at the Fermi surface and thus there still exists a residual Fermi surface for weak Coulomb correlations. However for $\mu = 3$, the residual Fermi surface disappears completely. This result is in agreement with the analytical observation of Lieb and Mattis.

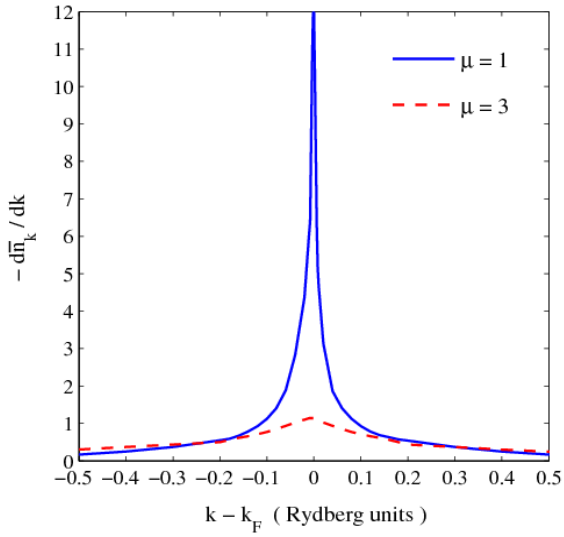

Fig. 2.4 Variation of $\left[-\frac{d\bar{n}_k}{dk}\right]$ as a function of $(k - k_F)$.

In Fig. 2.5 we show the behavior of the momentum distribution of the electrons in a FTL liquid i.e., when both the acoustic and optical electron-phonon interactions are present in the LL. For the sake of comparison, we plot the distribution function for the electrons for three cases, namely, for $\mu = 1,\ \alpha_{ac} = 0,\ \alpha_{op} = 0;\ \mu = 1,\ \alpha_{ac} = 2.2,\ \alpha_{op} = 0,$ and $\mu = 1,\ \alpha_{ac} = 2.2,\ \alpha_{op} = 0.35$. It is clear that like electron-electron interaction, electron-phonon interactions also flatten the distribution function, the optical-phonons, of course, having a larger effect than the acoustic-phonons. It is also evident that the nature of the residual Fermi surface of a FTL liquid is more or less the same as that of the corresponding LL. It is important to note that in the presence of electron-phonon interactions, the distribution function has a rather long tail which remains more or less unaffected by the coupling constants, particularly for low-lying excitations. Thus the behavior

of the distribution function of a FTL liquid is qualitatively different from that of a LL above k_F.

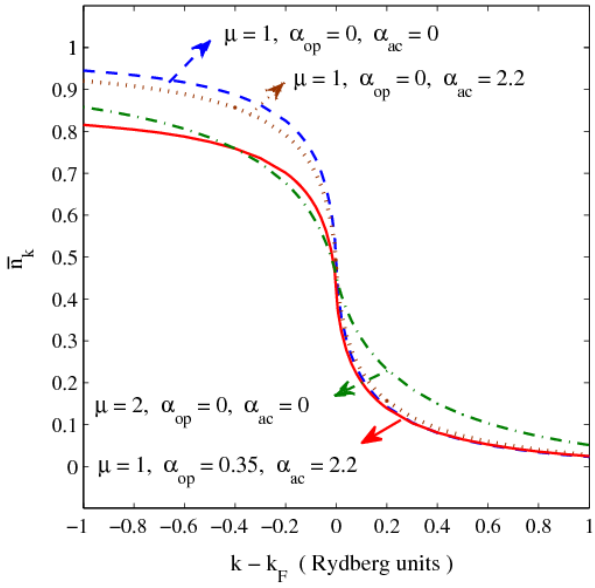

Fig. 2.5 Momentum distribution function of the FTL liquid.

2.5 Conclusions

In conclusion, we have studied the momentum distribution function for the electrons in a LL in the presence of both electron-acoustic- phonon and electron-optical-phonon interactions. Such a system can be referred to as an FTL liquid. We have shown that in the case of a LL strong Coulomb interactions destroy the residual Fermi surface completely. We find that in the case of an FTL liquid, the residual Fermi system is also destroyed by the electron-phonon interactions. Furthermore, the optical-phonon interaction is observed to have a larger effect on the distribution function than the

acoustic-phonon interaction. Interestingly enough, the distribution function has a very long tail above k_F in an FTL liquid, which is apparently unaffected by the strengths of the electron-phonon interactions. Thus the momentum distribution function an FTL liquid shows a qualitatively different behavior from that of a LL above k_F particularly for low-lying excitations.

References

[1] J. M. Luttinger, *J. Math. Phys*. **4**, 1154 (1963).

[2] B. Dardel *et al*., *Europhys. Lett.* **24**, 687 (1993);
M. Bockrath *et al*., *Nature* **397**, 598 (1999);
S. Sen and S. Chakrabarti, *Physica E* **40**, 2736 (2008).

[3] P. W. Anderson and Y. R. Ren, *Proceedings of the Los Alamos Conference on High-T_c Superconductivity*, Addison Wesley Publ. Comp., 1990, p. 3;
P. W. Anderson, *Phys. Rev. Lett.* **64**, 1839 (1990);
P. W. Anderson, *Phys. Rev. Lett.* **65**, 2306 (1990).

[4] F. Bloch *Helv. Phys. Acta* **7**, 385 (1934).

[5] S.Tomonaga, *Prog. Theor. Phys.*(*Kyoto*) **5**, 544 (1950).

[6] D. C. Mattis and E. H. Lieb, *J. Math. Phys.* **6**, 304 (1965).

[7] A. Luther and I. Peschel, *Phys. Rev. B* **9**, 2911 (1974).

[8] F. D. M. Haldane, *J. Phys. C* **14**, 2585 (1981).

[9] D. Yoshioka and M. Ogata, *J. Phys. Soc. Jpn.* **9,** 2990 (1993).

[10] J. M. Calleja *et al.*, *Solid State Commun.* **79**, 911 (1991).

[11] B. Y. Hu and S. Das Sarma, *Phys. Rev. Lett.* **68**, 1750 (1992); *ibid*, *Phys. Rev B* **48**, 5469 (1993).

[12] A. A. Melgarejo and F. Vericat, *Physica E* **8**, 57 (2000).

[13] W. Wonneberger, *Phys. Rev. A* **63**, 063607 (2001).

[14] D. W. Wang, A. J. Millis and S. Das Sarma, *Phys. Rev. B* **64**, 193304 (2001).

[15] K. Schönhammer, *J. Phys. Condens. Matt,* **14**, 12783 (2002).

[16] S. Sen and S. chakrabarti, *Physica E* **40**, 2736 (2008).

[17] R. Egger *et al*., 'Luttinger liquid behavior in metallic carbon nanotubes', in *Interacting Electrons in Nanostructures*, edited by R. Haug and H. Schoeller (Springer Verlag, Berlin, 2001).

[18] G. Whitfield and P. B. Shaw, *Phys. Rev. B* **14,** 3346 (1976);
F. M. Peeters and J. T. Devreese, *Phys. Rev. B* **36**, 4442 (1987);
T. K. Mitra, A. Chatterjee and S. Mukhopadhyay, *Phys. Rep.* **153**, 91 (1987);
J. Voit and H. J. Schulz, *Phys. Rev. B* **36**, 968 (1987).

[19] I. Baldea , *Physica Sripta* **31**, 606 (1985).

[20] E. C. Marino, *Phys. Rev. Lett.* **55**, 2991 (1985).

[21] M. J. Martins, *J. Phys. C* **20**, L765 (1987).

[22] C. S. Rao, P. M. Krishna, S. Mukhopadhyay and A. Chatterjee, *J. Phys.: Condens. Matter* **13**, L919 (2001).

[23] M. H. Degani, O. Hipolito, R. Lobo and G. A. Farias, *J. Phys. C* **19**, 2919 (1986).

Chapter 3

Persistent current in a Holstein-Hubbard ring in the presence of Rashba spin-orbit interaction

3.1 Introduction

When a charged particle moves along a closed path around a flux tube its wave function picks up a phase even though the magnetic field is zero. This is called the Aharonov-Bohm (AB) effect. Here we consider the magnetic flux going through the quantum ring (QR) in such a way that the magnetic field is zero at the radius of the ring. It is a quantum mechanical phenomenon which can be observed in small metallic rings whose size is comparable to the electron coherence length. The energy spectrum is periodic in flux and consequently, the persistent current (PC) which is the change in ground state (GS) energy with respect to the magnetic flux is also periodic in flux. Actually, the AB effect illustrates the physicality of electromagnetic potentials φ and A. In Feynman's path integral view of dynamics the potential field directly changes the phase of an electron wave function and these changes in the phase leads to measurable quantities.

The existence of PC in a normal metal ring was first proposed by Buttiker, Imry and Landauer [1]. Cheung et al. [2] have studied the effects of temperature, chemical potential and randomness on PC in strictly one-

dimensional (1D) normal rings. Several theoretical studies [3] have been subsequently carried out on PC in mesoscopic systems. With the advent of nano-fabrication techniques, several experimental investigations have been made to confirm the existence [4] and the periodicity [5] of PC in semiconductor quantum rings (QR's). The periodicity of PC in a finite ring can be shown using continuum or discrete models [6]. The period is found to be $\Phi_0 = hc/e$ for non-interacting spinless electrons. The most useful model to study PC is the Hubbard model in which the ring consists of discrete lattice sites and the electrons can hop from one site to another. Several works [7] have been carried out on the Hubbard ring to understand the magnetic response and the behaviour of PC. But most of them have neglected the electron-phonon interaction which can actually play quite an important role in the low-dimensional systems. The effect of electron-phonon interaction on PC can be captured by considering the Holstein-Hubbard (HH) model [8].

3.1.1 Spin-orbit interaction

Another important interaction that has come to light in the context of nanosystems in recent years is the spin-orbit (SO) interaction which is at the heart of the emerging field of spintronics. New devices are being contemplated based purely on the spin degrees freedom instead of charge. The effects of SO interaction [9] are found to be pronounced in QR's. There are two microscopic origins for the SO interactions. One originates due to the structural inversion asymmetry which is known as the Rashba spin-orbit (RSO) interaction and the other is due to the bulk inversion asymmetry which is known as the Dresselhaus spin-orbit (DSO) interaction. The Rashba effect makes it possible to control the electron spin by the external

electric field which is precisely the idea behind spintronics [10]. In the present paper we shall study the effects of RSO interaction on PC in a 1D HH ring threaded by an AB flux.

Since the number of electrons in a QR also changes the magnitude and phase of PC [2], the chemical potential is expected to have an interesting effect on PC. As the temperature increases, the electrons may occupy higher energy levels which are close and can have opposite currents and therefore, as a net result, the higher positive and negative contributions to PC may cancel out. Buttiker has indeed observed a decrease in the amplitude of the PC with temperature [11]. We shall therefore study the effects of chemical potential and temperature as well on PC in a 1D HH ring in the presence of RSO interaction.

3.2 Theoretical Formalism

The Hamiltonian for a HH ring threaded by a magnetic flux Φ can be written in the presence of RSO interaction as:

$$H = H_{el} + H_p + H_{ep} + H_{so} , \tag{3.1}$$

where

$$H_{el} = \varepsilon_0 \sum_i c_i^\dagger c_i - t\, e^{i\theta} \sum_{\langle ij \rangle} \left[c_i^\dagger c_j + h.c \right] + U \sum_i n_{i\uparrow} n_{i\downarrow} , \tag{3.2}$$

$$H_p = \hbar\omega_0 \sum_i \left(b_i^\dagger\, b_i + {}^1/_2 \right) , \tag{3.3}$$

$$H_{ep} = g_1 \sum_i n_i \left(b_i + b_i^\dagger\right) + g_2 \sum_{\langle ij \rangle} n_i \left(b_j + b_j^\dagger\right), \tag{3.4}$$

$$H_{so} = -\sum_{\langle ij \rangle} \left[c_i^\dagger \, t_{so} \, e^{i\theta} \, c_j + h.c \right]. \tag{3.5}$$

Eqn. (3.2) represents the electronic Hamiltonian H_{el} which consists of three terms. The first term represents the site energy, ε_0 being the onsite energy, $c_i = \begin{pmatrix} c_{i\uparrow} \\ c_{i\downarrow} \end{pmatrix}$, $c_{i\sigma}^\dagger \, (c_{i\sigma})$ being the creation (annihilation) operator for an electron at site i with spin σ, and $i = 1,2,3, \ldots N$, N being the total number of sites in the system. The second term describes the hopping term, where t is the hopping integral between the nearest-neighbour (NN) sites, $\langle ij \rangle$ denotes that the summation is to be performed over NN sites i and j and $\theta = (2\pi\Phi/\mathrm{N})$ is the AB phase due to the magnetic flux Φ, which is an integral multiple of the elementary flux quantum $\Phi_0 = hc/e$. The third term is the onsite repulsive electron-electron Coulomb interaction where U measures the strength of the interaction and $n_{i\sigma} = c_{i\sigma}^\dagger \, c_{i\sigma}$ is the number operator for the electrons at site i with spin σ. Eqn. (3.3) gives the unperturbed phonon Hamiltonian, where $b_i^\dagger \, (b_i)$ is the creation (annihilation) operator for a phonon with dispersionless frequency ω_0 at site i. Eqn. (3.4) represents the on-site and NN electron-phonon interactions with g_1 and g_2 measuring the respective coupling constants. Thus g_1 measures the strength of the interaction of an electron with the phonons at the i-th site, whereas g_2 gives the strength of the interaction of an electron at the i-th site with the phonons at the $(i+1)$-th site. The value of g_2 is in general expected to be smaller than that of g_1 and typically for a real material one may take the value of g_2 about one order less than that of g_1. In general, an electron is supposed to interact with phonons at all sites. But

we restrict our study of electron-phonon interaction up to NN terms assuming that beyond NN's, interactions will so small that they can be ignored. [If the onsite electron-phonon interaction is so strong that the electron gets trapped in a deep potential well created at the i-th site, then its interaction with the NN phonons will be very small. In such cases the effective NN electron-phonon interaction can be neglected]. In real systems the effects of g_1 and g_2 manifest themselves through the localization-delocalization transition. Finally, Eqn. (3.5) describes the SO interaction with

$$t_{so} = i\alpha\left(\sigma_x \cos\varphi_{ij} + \sigma_y \sin\varphi_{ij}\right) - i\beta\left(\sigma_y \cos\varphi_{ij} + \sigma_x \sin\varphi_{ij}\right), \quad (3.6)$$

where $\varphi_i = 2\pi(i-1)/N$ so that $\varphi_{ij} = \left(\varphi_i + \varphi_j\right)/2 = 2\pi\left(i - \frac{1}{2}\right)/N$, σ_x and σ_y are the Pauli spin matrices, and $i(= 1,2,\dots,N)$ is the site index along the azimuthal direction φ of the ring. In the present problem we are interested in the RSO interaction only and so we take $\beta = 0$.

First we perform the Lang-Firsov transformation (LFT) [12] which works well in the strong-coupling limit. We carry out LFT with the generator

$$R = \frac{1}{\hbar\omega_0}\left[g_1 \sum_{i\sigma} n_{i\sigma}\left(b_i^\dagger - b_i\right) + g_2 \sum_{\langle ij\rangle\sigma} n_{i\sigma}\left(b_j^\dagger - b_j\right)\right] \quad (3.7)$$

followed by the zero-phonon averaging to get an effective Hamiltonian

$$H_{eff} = \langle 0|e^R H e^{-R}|0\rangle \quad (3.8)$$

Now let us write our Hamiltonian as

$$H = H_1 + H_2 + H_3 + H_4 + H_5 + H_6 + H_7 \,. \tag{3.9}$$

with

$$H_1 = \sum_i c_i^+ \epsilon_0 c_i \,, \tag{3.10}$$

$$H_2 = -t \sum_{\langle ij\rangle\sigma} c_{i\,\sigma}^+ c_{j\,\sigma}\, e^{i\theta} + h.c \,, \tag{3.11}$$

$$H_3 = -i \sum_{\langle ij\rangle\sigma} c_{i\,\sigma}^+ \begin{bmatrix} 0 & P \\ Q & 0 \end{bmatrix} c_{j\,\sigma}\, e^{i\theta} \,, \quad P = \alpha e^{-i\varphi_{ij}}, \qquad Q = \alpha e^{i\varphi_{ij}}, \tag{3.12}$$

$$H_4 + H_5 = g_1 \sum_{i\sigma} n_{i\sigma}(b_i + b_i^+) + g_2 \sum_{\langle ij\rangle\sigma} n_{i\sigma}\left(b_j + b_j^+\right) \,, \tag{3.13}$$

$$H_6 = \hbar\omega_0 \sum_i \left(b_i^+ b_i + {}^1\!/_2\right) \,, \tag{3.14}$$

$$H_7 = U \sum_i n_{i\uparrow} n_{i\downarrow} \,. \tag{3.15}$$

We recall,

$$\widetilde{H} = e^R H e^{-R} = H + [R,H] + \frac{1}{2!}\big[R,[R,H]\big] + \cdots \,. \tag{3.16}$$

Thus we obtain

$$\widetilde{H}_1 = e^R\, H_1\, e^{-R} = H_1 \,, \tag{3.17}$$

$$\widetilde{H}_2 = e^R\, H_2 e^{-R} = -t e^{i\theta} \sum_{\langle ij\rangle\sigma} e^{(Y_i - Y_j)} c_{i\,\sigma}^+ c_{j\,\sigma} \,, \tag{3.18}$$

with

$$Y_i = \frac{g_1}{\hbar\omega_0}(b_i^+ - b_i) + \frac{g_2}{\hbar\omega_0}\sum_{\delta'}\left(b_{i+\delta'}^+ - b_{i+\delta'}\right), \tag{3.19}$$

$$\widetilde{H}_3 = e^R H_3 e^{-R} = -ie^{i\theta}\sum_{\langle ij\rangle\sigma}\begin{bmatrix}0 & P\\ Q & 0\end{bmatrix} e^{(Y_i - Y_j)} c_{i\sigma}^+ c_{j\sigma}, \tag{3.20}$$

$$\widetilde{H}_4 + \widetilde{H}_5 = e^R(H_4 + H_5)e^{-R}$$

$$= g_1\sum_{i\sigma} n_{i\sigma}(b_i + b_i^+) + g_2\sum_{\langle ij\rangle\sigma} n_{i\sigma}\left(b_j + b_j^+\right) - \frac{2}{\hbar\omega_0}({g_1}^2 + z\,{g_2}^2)\sum_{i\sigma} n_{i\sigma}$$
$$- \frac{4}{\hbar\omega_0}({g_1}^2 + z\,{g_2}^2)\sum_i n_{i\uparrow}n_{i\downarrow} - \frac{2\,{g_2}^2}{\hbar\omega_0}\sum_{i\Delta\sigma\sigma'} n_{i\sigma}n_{i+\Delta\,\sigma'}$$
$$- \frac{2}{\hbar\omega_0}(g_1g_2 + g_2g_1)\sum_{\langle ij\rangle\,\sigma\sigma'} n_{i\sigma}n_{j\sigma'}, \tag{3.21}$$

$$\widetilde{H}_6 = e^R H_6\, e^{-R}$$

$$= \hbar\omega_0\sum_i\left(b_i^+ b_i + {}^1\!/_2\right) - g_1\sum_{i\sigma} n_{i\sigma}(b_i + b_i^+) - g_2\sum_{\langle ij\rangle\sigma} n_{i\sigma}\left(b_j + b_j^+\right)$$

$$+ \frac{1}{2!}\left\{\frac{2}{\hbar\omega_0}({g_1}^2 + z\,{g_2}^2)\sum_{i\sigma} n_{i\sigma} + \frac{4}{\hbar\omega_0}({g_1}^2 + z\,{g_2}^2)\sum_i n_{i\uparrow}n_{i\downarrow}\right.$$
$$\left. + \frac{2{g_2}^2}{\hbar\omega_0}\sum_{i\Delta\sigma\sigma'} n_{i\sigma}n_{i+\Delta\,\sigma'} + \frac{4g_1g_2}{\hbar\omega_0}\sum_{\langle ij\rangle\,\sigma\sigma'} n_{i\sigma}\,n_{j\sigma'}\right\}, \tag{3.22}$$

$$\widetilde{H}_7 = e^R H_7\, e^{-R} = H_7\,. \tag{3.23}$$

Thus the transformed Hamiltonian $\widetilde{H}$ is given by

$$\widetilde{H} = \left[-\frac{1}{\hbar\omega_0}({g_1}^2 + z\,{g_2}^2)\right]\sum_{i\sigma} n_{i\sigma} - \; te^{i\theta}\sum_{\langle ij\rangle\sigma}\; e^{(Y_i - Y_j)}c_{i\,\sigma}^{+}c_{j\,\sigma}$$

$$- ie^{i\theta}\sum_{\langle ij\rangle\sigma}\begin{bmatrix}0 & P\\ Q & 0\end{bmatrix} e^{(Y_i - Y_j)}c_{i\,\sigma}^{+}c_{j\,\sigma} \; + \left[U - \frac{2}{\hbar\omega_0}({g_1}^2 + z\,{g_2}^2)\right]\sum_{i} n_{i\uparrow}n_{i\downarrow}$$

$$-\frac{2g_2\,g_1}{\hbar\omega_0}\sum_{\langle ij\rangle\,\sigma\sigma'} n_{i\sigma}n_{j\sigma'} - \frac{{g_2}^2}{\hbar\omega_0}\sum_{i\Delta\sigma\sigma'} n_{i\sigma}n_{i+\Delta\,\sigma'} + \hbar\omega_0\sum_{i}\left(b_i^{+}b_i + \frac{1}{2}\right). \quad (3.24)$$

The zero-phonon averaging of $\widetilde{H}$ gives the effective electronic Hamiltonian H_{eff} i.e.,

$$H_{eff} = \langle 0|\widetilde{H}|0\rangle \; . \quad (3.25)$$

We can easily see that $[Y_j\,, Y_i] = 0$ and

$$\langle 0|e^{Y_i - Y_j}|0\rangle = e^{-\left(\frac{1}{\hbar\omega_0}\right)^2[(g_1 - g_2)^2 + (z-1)g_2{}^2]} \; . \quad (3.26)$$

Using the above results, the effective electronic Hamiltonian can be written in a simplified form:

$$H_{eff} = \epsilon_0{}^{e}\sum_{i\sigma} n_{i\sigma} - t_e\, e^{i\theta}\sum_{\langle ij\rangle\sigma} c_{i\sigma}^{+}c_{j\sigma} - t_{SO-e}^{ij}\, e^{i\theta}\sum_{\langle ij\rangle\sigma} c_{i\sigma}^{+}c_{j\sigma}$$

$$+ U_e\sum_{i} n_{i\uparrow}n_{i\downarrow} \; , \quad (3.27)$$

where

$$\epsilon_0^e = -\frac{(\,g_1^2 + z\;g_2^2)}{\hbar\omega_0} \; , \qquad (z = \text{number of NNs}) \quad (3.28)$$

$$t_e \; = t\, e^{-[\,(g_1 - g_2)^2 + (z-1)\,g_2{}^2\,]/(\hbar\omega_0)^2} \; , \quad (3.29)$$

$$t_{SO-e}^{ij} = \boldsymbol{i}\,\mathbb{A}\, e^{-[\,(g_1-g_2)^2+(z-1)\,g_2{}^2\,]/(\hbar\omega_0)^2}\,, \tag{3.30}$$

$$\mathbb{A} = \begin{bmatrix} 0 & P \\ Q & 0 \end{bmatrix} = \begin{bmatrix} 0 & \alpha\ e^{-\boldsymbol{i}\,\varphi_{ij}} \\ \alpha\ e^{\boldsymbol{i}\,\varphi_{ij}} & 0 \end{bmatrix}, \tag{3.31}$$

$$U_e = U - \frac{2}{\hbar\omega_0}(\,\mathrm{g}_1^2 + z\,\mathrm{g}_2^2\,)\ . \tag{3.32}$$

Now we perform a unitary transformation on H_{eff} with the matrix

$$U_m = \frac{1}{\sqrt{2}} \begin{bmatrix} 1 & -1 \\ e^{\frac{2\pi\boldsymbol{i}}{N}\left(m-\frac{1}{2}\right)} & e^{\frac{2\pi\boldsymbol{i}}{N}\left(m-\frac{1}{2}\right)} \end{bmatrix} \tag{3.33}$$

to eliminate the index dependence on the SO term t_{SO-e}^{ij}. This transforms the old operators c_i to a new set of operators $\tilde{c}_i = U_i{}^{+} c_i$ and the transformed Hamiltonian H_e reads

$$H_e = \epsilon_0^e \sum_{i\sigma} \tilde{n}_{i\sigma} - \frac{1}{2}\, e^{\boldsymbol{i}\,\theta} \sum_{\langle ij\rangle\sigma} \tilde{c}_{i\,\sigma}^{\dagger}\,[t_e + \boldsymbol{i}\,\alpha_e]\mathbb{B}\,\tilde{c}_{j\,\sigma} + U_e \sum_i \tilde{n}_{i\uparrow}\,\tilde{n}_{i\downarrow}$$

$$+ \frac{\tilde{n}_i\left[\tilde{c}_{i\uparrow}^{\dagger}\,\tilde{c}_{i\downarrow} + \tilde{c}_{i\downarrow}^{\dagger}\,\tilde{c}_{i\uparrow}\right]}{4} - \frac{\left[\tilde{c}_{i\uparrow}^{\dagger}\,\tilde{c}_{i\downarrow} + \tilde{c}_{i\downarrow}^{\dagger}\,\tilde{c}_{i\uparrow}\right]\tilde{n}_i}{4}\,, \tag{3.34}$$

where,

$$\alpha_e = \alpha\ \mathrm{e}^{-[\,(g_1-g_2)^2+(z-1)\,g_2{}^2\,]/(\hbar\omega_0)^2}\,, \tag{3.35}$$

$$\mathbb{B} = \begin{bmatrix} 1+e^{\frac{2\pi\boldsymbol{i}}{N}} & -1+e^{\frac{2\pi\boldsymbol{i}}{N}} \\ -1+e^{\frac{2\pi\boldsymbol{i}}{N}} & 1+e^{\frac{2\pi\boldsymbol{i}}{N}} \end{bmatrix}. \tag{3.36}$$

We use the mean-field approximation (MFA) to linearize the quadratic terms in H_e. In 1D systems, for a half filled band the electron-phonon interaction can cause distortion of the lattice leading to the dimerization

with the unit cell getting doubled. We divide the lattice into two sublattices: even numbered sites-A and odd numbered sites-B. Then, some algebraic simplifications following Cabib and Callen [13] gives,

$$H_e^M = \sum_{i=1}^{N} \tilde{c}_i^{\dagger}[\,\mathbb{C} + (-1)^i \mathbb{D}]\,\tilde{c}_i - e^{i\left(\theta+\frac{\pi}{N}\right)} \sum_{\langle ij\rangle\sigma}^{N} \tilde{c}_{i\sigma}^{\dagger}\,[t_e\mathbb{E} + \boldsymbol{i}\alpha_e\mathbb{F}]\tilde{c}_{j\sigma} + K, \tag{3.37}$$

where,

$$\mathbb{C} = \begin{bmatrix} \varepsilon_{AB\uparrow}^{+} & 0 \\ 0 & \varepsilon_{AB\downarrow}^{+} \end{bmatrix}, \tag{3.38}$$

$$\varepsilon_{AB\uparrow}^{+} = \frac{\varepsilon_{A\uparrow} + \varepsilon_{B\uparrow}}{2} \quad \text{and} \quad \varepsilon_{AB\downarrow}^{+} = \frac{\varepsilon_{A\downarrow} + \varepsilon_{B\downarrow}}{2}, \tag{3.39}$$

$$\mathbb{D} = \begin{bmatrix} \varepsilon_{AB\uparrow}^{-} & 0 \\ 0 & \varepsilon_{AB\downarrow}^{-} \end{bmatrix}, \tag{3.40}$$

$$\varepsilon_{AB\uparrow}^{-} = \frac{\varepsilon_{A\uparrow} - \varepsilon_{B\uparrow}}{2} \quad \text{and} \quad \varepsilon_{AB\downarrow}^{-} = \frac{(\varepsilon_{A\downarrow} - \varepsilon_{B\downarrow})}{2}, \tag{3.41}$$

with

$$\varepsilon_{A\uparrow} = \epsilon_0^e + \frac{U_e(c-s)}{2} \quad \text{and} \quad \varepsilon_{B\uparrow} = \epsilon_0^e - \frac{U_e(c-s)}{2}, \tag{3.42}$$

$$\varepsilon_{A\downarrow} = \epsilon_0^e + \frac{U_e(c+s)}{2} \quad \text{and} \quad \varepsilon_{B\downarrow} = \epsilon_0^e - \frac{U_e(c+s)}{2}, \tag{3.43}$$

$$\mathbb{E} = \begin{bmatrix} cos(\pi/N) & \boldsymbol{i}\ sin(\pi/N) \\ \boldsymbol{i}\ sin(\pi/N) & cos(\pi/N) \end{bmatrix}, \tag{3.44}$$

$$\mathbb{F} = \begin{bmatrix} cos(\pi/N) & \boldsymbol{i}\ sin(\pi/N) \\ -\boldsymbol{i}\ sin(\pi/N) & -cos(\pi/N) \end{bmatrix}, \tag{3.45}$$

and

$$K = \frac{NU_e(n^2 - c^2 + s^2)}{4} \ , \tag{3.46}$$

$$n = \frac{[(n_{A\uparrow} + n_{A\downarrow}) + (n_{B\uparrow} + n_{B\downarrow})]}{2} \ , \tag{3.47}$$

$$c = \frac{[(n_{A\uparrow} + n_{A\downarrow}) - (n_{B\uparrow} + n_{B\downarrow})]}{2} \ , \tag{3.48}$$

$$s = \frac{[(n_{A\uparrow} - n_{A\downarrow}) - (n_{B\uparrow} - n_{B\downarrow})]}{2} \ , \tag{3.49}$$

where n- electron concentration, c- charge density wave (CDW) order parameter and s- spin density wave (SDW) order parameter. Using the Fourier transform:

$$\tilde{c}_{m\sigma} = \frac{1}{\sqrt{N}} \sum_k e^{ikma} \ \tilde{c}_{k\sigma} \ , \tag{3.50}$$

where a is the lattice constant and redefining $\tilde{c}_{i\sigma}$ ($\tilde{c}^{\dagger}_{i\sigma}$) as $c_{i\sigma}$ ($c^{\dagger}_{i\sigma}$) and $\tilde{c}_{k\sigma}(\tilde{c}^{\dagger}_{k\sigma})$ as $c_{k\sigma}$ ($c^{\dagger}_{k\sigma}$) and separating the Hamiltonian into even and odd sited terms using the following identities,

$$\sum_{m=1}^{N/2} c^{+}_{2m} \, c_{2m} = \frac{1}{2}\sum_k c^{+}_k c_k + \frac{1}{2}\sum_k c^{+}_k c_{k+\frac{\pi}{a}} \quad , for \ even \ sites, \tag{3.51}$$

$$\sum_{m=1}^{N/2} c^{+}_{2m-1} \, c_{2m-1} = \frac{1}{2}\sum_k c^{+}_k c_k - \frac{1}{2}\sum_k c^{+}_k c_{k+\frac{\pi}{a}} \quad , for \ odd \ sites, \tag{3.52}$$

we get the effective mean-field Hamiltonian after some rearrangement of the terms as:

$$H_e^M = \sum_{k=-\pi/a}^{\pi/a} c_k^\dagger \, \mathbb{G} \, c_k \; + \sum_{k=-\pi/a}^{\pi/a} c_k^\dagger \, \mathbb{H} \, c_{k+(\pi/a)} + K \; , \qquad (3.53)$$

where,

$$\mathbb{G} = \begin{bmatrix} \varepsilon_{AB\uparrow}^{+} + \alpha_{11} & \alpha_{12} \\ \alpha_{21} & \varepsilon_{AB\downarrow}^{+} + \alpha_{22} \end{bmatrix}, \qquad (3.54)$$

$$\mathbb{H} = \begin{bmatrix} \varepsilon_{AB\uparrow}^{-} & 0 \\ 0 & \varepsilon_{AB\downarrow}^{-} \end{bmatrix} , \qquad (3.55)$$

$$\alpha_{11} = -2\, t_e \; cos(\pi/N)\, cos(ka + \theta + \pi/N) + \; 2\, \alpha_e \; cos(\pi/N)\, sin(ka + \theta + \pi/N) \; , \qquad (3.56)$$

$$\alpha_{12} = 2\, t_e \; sin(\pi/N)\, sin(ka + \theta + \pi/N) + \; 2\, \alpha_e \; sin(\pi/N)\, cos(ka + \theta + \pi/N) \; , \qquad (3.57)$$

$$\alpha_{21} = 2\, t_e \; sin(\pi/N)\, sin(ka + \theta + \pi/N) - \; 2\, \alpha_e \; sin(\pi/N)\, cos(ka + \theta + \pi/N) \, , \qquad (3.58)$$

$$\alpha_{22} = -2\, t_e \; cos(\pi/N)\, cos(ka + \theta + \pi/N) - \; 2\alpha_e \, cos(\pi/N)\, sin(ka + \theta + \pi/N) \, . \qquad (3.59)$$

We shall work in the reduced zone scheme i.e., we choose k to lie in the range: $-\pi/2a \leq k \leq \pi/2a$. In this scheme, the matrix elements $\alpha's$ can be written as:

$$\alpha_{ij}(k+\pi/a) = -\alpha_{ij}(k)\,. \tag{3.60}$$

The effective mean-field Hamiltonian can now be written as:

$$H_e^M = \sum_{k=0}^{\pi} \left(c_{k\uparrow}^{\dagger}\ c_{k\downarrow}^{\dagger}\ c_{k+\pi,\uparrow}^{\dagger}\ c_{k+\pi,\downarrow}^{\dagger}\right)\ \mathbb{W} \begin{pmatrix} c_{k\uparrow} \\ c_{k\downarrow} \\ c_{k+\pi,\uparrow} \\ c_{k+\pi,\downarrow} \end{pmatrix}, \tag{3.61}$$

where

$$\mathbb{W} = \begin{bmatrix} \varepsilon_{AB\uparrow}^{+} + \alpha_{11} & \alpha_{12} & \varepsilon_{AB\uparrow}^{-} & 0 \\ \alpha_{21} & \varepsilon_{AB\downarrow}^{+} + \alpha_{22} & 0 & \varepsilon_{AB\downarrow}^{-} \\ \varepsilon_{AB\uparrow}^{-} & 0 & \varepsilon_{AB\uparrow}^{+} - \alpha_{11} & -\alpha_{12} \\ 0 & \varepsilon_{AB\downarrow}^{-} & -\alpha_{21} & \varepsilon_{AB\downarrow}^{+} - \alpha_{22} \end{bmatrix}. \tag{3.62}$$

The exact numerical diagonalization of H_e^M yields four energies E_1, E_2, E_3, E_4 and the four distribution functions $f(E_1), f(E_2),\ f(E_3), f(E_4)$, where

$$f(E_i) = \frac{1}{[e^{\beta\,(E_i-\mu)} + 1]}\ . \tag{3.63}$$

The GS energy is now given by,

$$E_{GS} = \sum_i E_i\ f(E_i) + K \tag{3.64}$$

The PC (I_{pc}) and the Drude weight (DW) can be calculated from the following relations:

$$I_{pc} = -\frac{1}{2\pi}\left(\frac{\partial E_{GS}}{\partial \Phi}\right), \tag{3.65}$$

$$DW = \frac{N}{4\pi^2}\frac{\partial^2 E_{GS}}{\partial \Phi^2}\bigg|_{\Phi=\Phi_m}, \tag{3.66}$$

where Φ_m is the location of the minimum of E_{GS} and can take values either 0 or $1/2$ depends on the parity of the number of electrons. DW is a good parameter to understand the conducting nature of the system which was first observed by Kohn [14].

3.3 Numerical results and Discussions

We set $t = 1$ and measure all energies in units of $\hbar\omega_0$. In Fig. 3.1, we plot

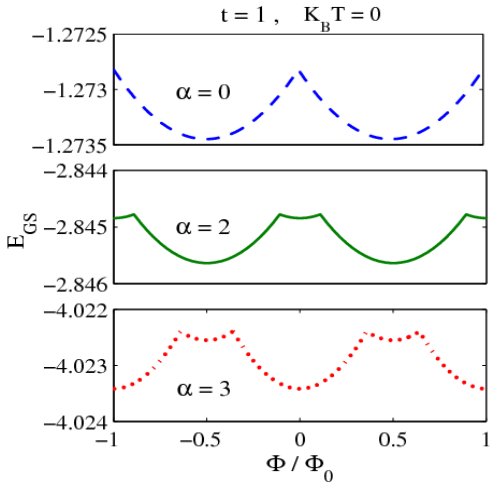

Fig. 3.1 The GS energy as a function of the flux Φ for different α.

the GS energy E_{GS} as a function of the flux Φ for various values of α in the absence of all other interactions. We can see that the GS energy increases with α. The periodicity of the energy with Φ is also clearly evident.

In Fig. 3.2 we plot PC vs. Φ for different values of α. The RSO interaction clearly enhances I_{pc}. Also, the phase of the PC changes when α exceeds a critical value (α_c). In the present case, $\alpha_c > 1$.

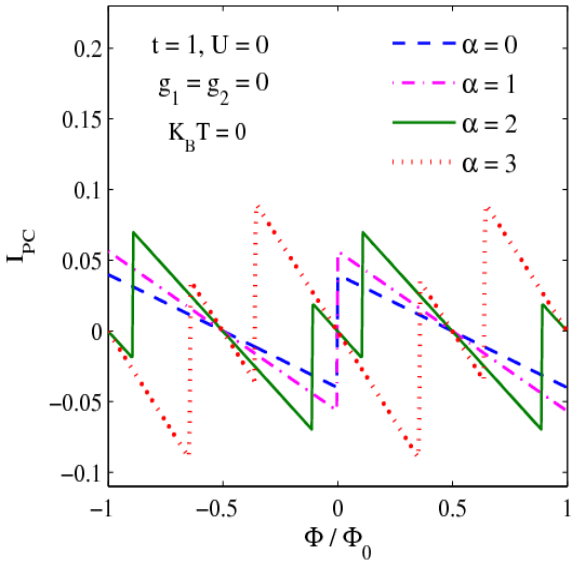

Fig. 3.2 Persistent current I_{PC} as a function of Φ for different α.

The variation of the PC (I_{PC}) as a function of the RSO interaction constant (α) is explicitly shown in Fig. 3.3. The increase of I_{PC} with α is monotonic, though its derivative can have an interesting behaviour.

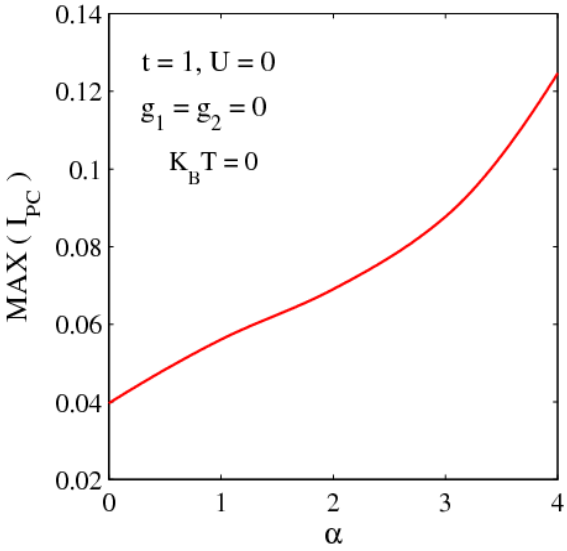

Fig. 3.3 Variation of I_{PC} as a function of α.

In Fig. 3.4, we plot the DW as a function of the flux Φ for various values of α in the absence of all other interactions. The finite value of the DW

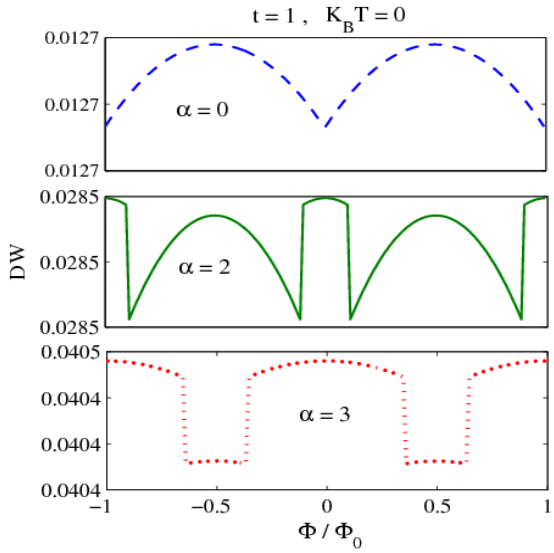

Fig. 3.4 Drude weight (DW) as a function of Φ for different α.

indicates that the system is in the metallic phase. We can see that the DW increases with α. The periodicity of DW with Φ also changes with the change in α.

3.3.1 Effect of electron-electron interaction

In Fig. 3.5 we plot PC as a function of Φ for different values of U in the presence of RSO interaction. It is clear that the PC decreases as U increases.

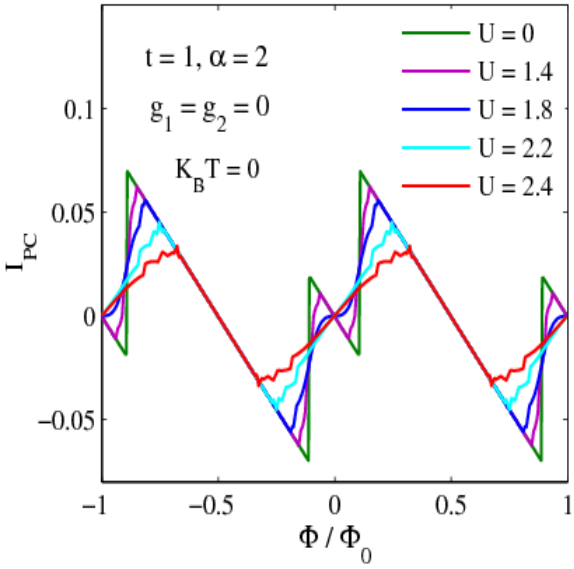

Fig. 3.5 I_{PC} vs. Φ for different values of U with $\alpha = 2$

The explicit form and the comparison of the behaviour of PC as a function of U with and without RSO interaction is shown in Fig. 3.6. The solid line describes the behaviour for $\alpha = 0$ and the dashed-dotted line for $\alpha = 2$. One can easily notice that PC decreases as U increases. The

explanation is quite simple. As U increases, the electrons experience a larger onsite repulsion and thus find it more difficult to go from one site to another. This reduces PC. In the absence of RSO interaction, there seems to exist some critical value of U (U_c) below which PC remains constant and unaffected by U. This implies that the effective hopping parameter t_e remains predominant over U below U_c. Above U_c, PC dies out extremely sharply. The behaviour is almost discontinuous. In the presence of RSO interaction, however, there is a qualitative difference in the behaviour of PC as a function of U. The $\alpha = 2$ curve in the figure shows that though, even now, the decrease of PC with increasing U is quite rapid, it is continuous and smooth and there is no indication of existence of any critical value of U.

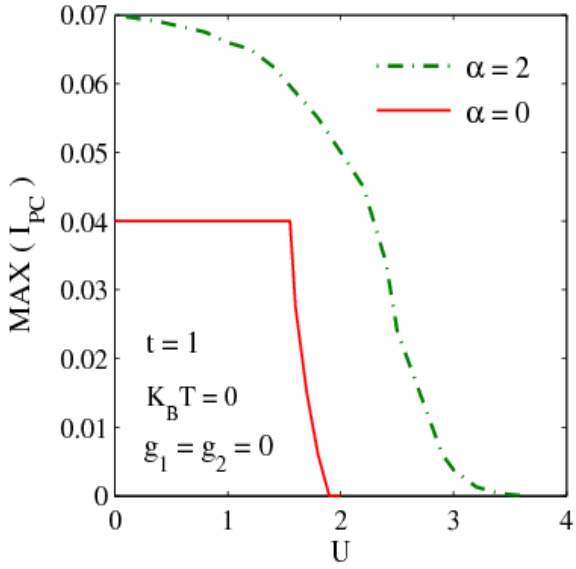

Fig. 3.6 I_{PC} as a function of U for $\alpha = 2$ and $\alpha = 0$.

3.3.2 Effect of electron-phonon interaction

Next, we look into the effects of on-site and NN electron-phonon interactions on PC. For that we have first switched off all other interactions and kept only the on-site electron-phonon interaction. The variation of PC as a function of Φ for different values of g_1 is shown in Fig. 3.7. It is clear that PC decreases as g_1 increases. This happens because increasing g_1 will lead to deepening of the self-trapping polarization potential causing localization which will inhibit conduction.

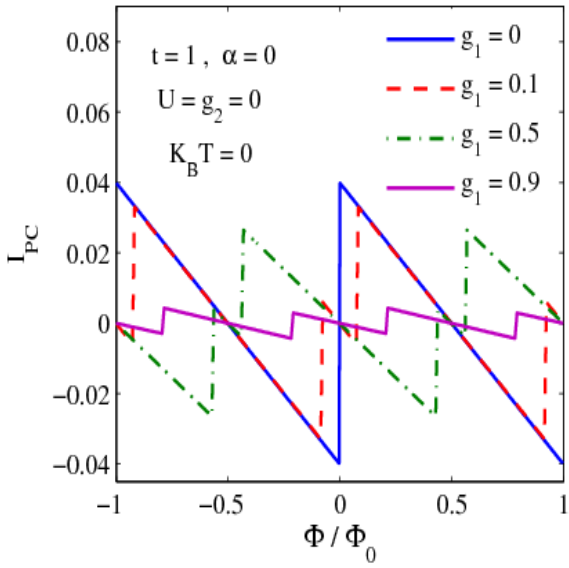

Fig 3.7: I_{PC} vs. Φ for different values of g_1 with $\alpha = 0$

To see the effects of g_1 on PC with and without RSO interaction we plot PC as a function of g_1 for $\alpha = 2$ and $\alpha = 0$ which is given in Fig. 3.8. It is evident that PC decreases as g_1 increases. Explanation for the reduction in PC with increasing g_1 is already given. The gradient of the curve is

however not monotonic which may have some interesting physical implications. One may also notice that the resistive effect of the electron-phonon interaction is more pronounced than that of the electron-electron interaction.

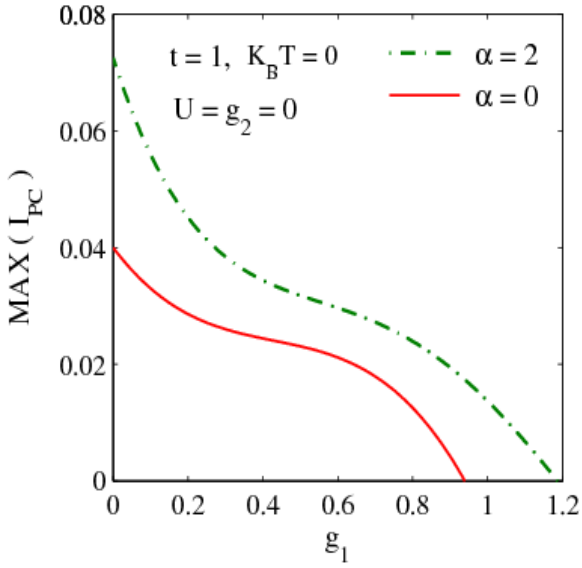

Fig. 3.8 I_{PC} vs. g_1 for $\alpha = 2$ and $\alpha = 0$ (with $U = 0 = g_2$).

In Fig. 3.9, we wish to study the effect of NN electron-phonon interaction on PC keeping $\alpha = 0$. So we plot I_{PC} vs. Φ for several values of g_2. To see the sole effect of g_2 we first study the case with $U = 0 = g_1$. We find that the effect of g_2 on PC is stronger than that of g_1, which is clearly suggested by Eqn. (3.29). According to Eqn. (3.29), t_e contains an additional Hoslstein reduction factor solely dependent on g_2. Fig 3.9 also shows that the periodicity of PC decreases with increasing g_2. The behaviour is qualitatively similar (not shown here) even with g_1, but again the effect of g_2 is stronger.

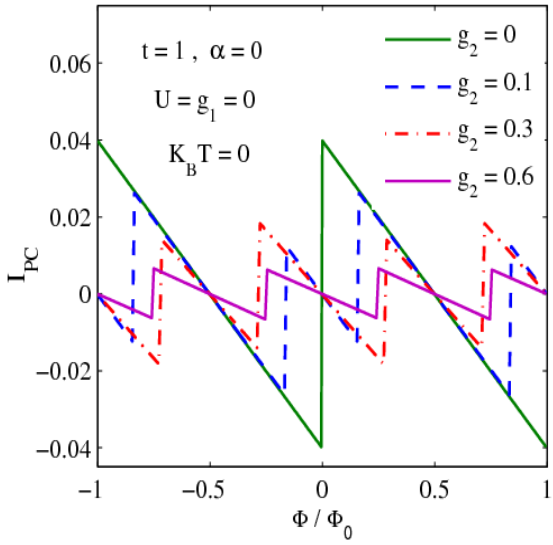

Fig. 3.9 I_{pc} vs. Φ for different values of g_2 with $\alpha = 0$.

In Fig. 3.10, we show PC vs. Φ for $g_2 = 0$ and 0.1 in the presence of on-site electron-phonon interaction ($g_1 = 0.9$). Of course, the reduction in

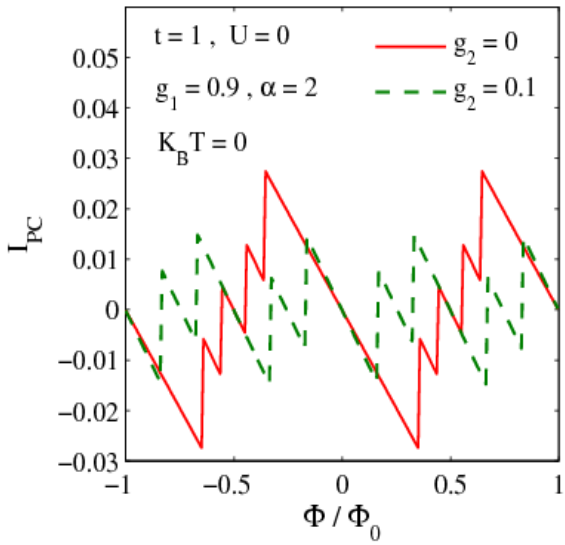

Fig. 3.10 I_{pc} vs. Φ for $g_2 = 0$ and 0.1 with $g_1 = 0.9$.

PC is now more pronounced and furthermore the periodicity also decreases. We do not plot PC vs. g_2 because the behaviour is infested with a lot of fluctuations.

3.3.3 Temperature effects

Next we are interested to study the effects of temperature on PC. So we have turn off all the interactions and plot the variation of PC as a function of Φ for different values of temperature in Fig. 3.11 for $\alpha = 0$. In Fig. 3.12, we plot PC vs. Φ for $\alpha = 2$. From both the figures we find that the PC decreases as temperature increases. As we have mentioned in the introduction, when the temperature increases the electrons may occupy higher energy levels which are close and can have opposite currents. As a net result, the higher positive and negative contributions to PC may cancel out. Hence the PC reduces.

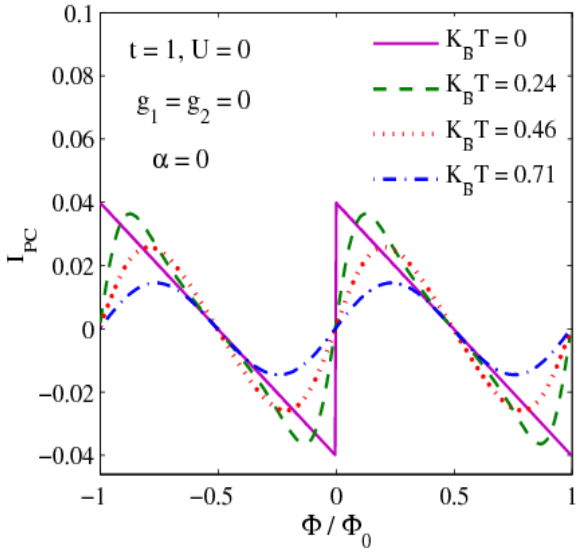

Fig. 3.11 I_{pc} vs. Φ for different values of K_BT with $\alpha = 0$.

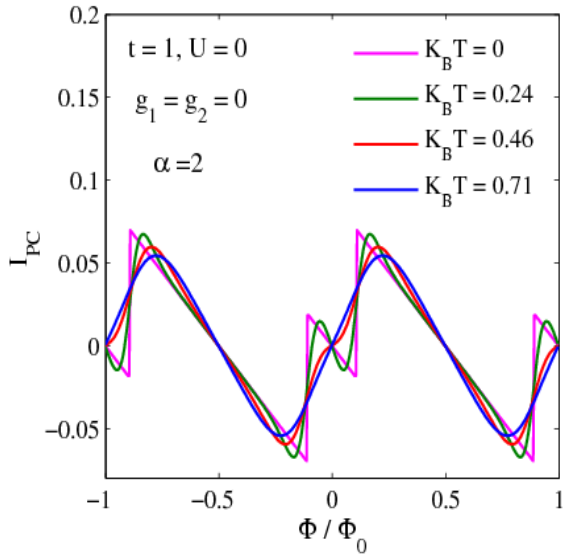

Fig. 3.12 I_{pc} vs. Φ for different values of K_BT with $\alpha = 2$.

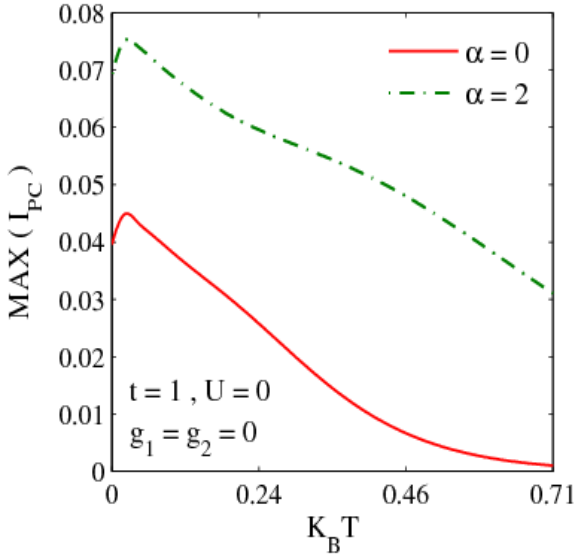

Fig 3.13: I_{pc} as a function of temperature for $\alpha = 0$ and $\alpha = 2$.

The effect of temperature on PC is plotted in Fig. 3.13 for both $\alpha = 0$ and $\alpha = 2$ and it is clear that as the temperature increases, PC decreases in both cases as our commonplace notion would justify. The exact numerical behaviour is however a little more complicated eluding any simple explanation. As established earlier, PC is larger in the presence of the RSO interaction. Interestingly enough, PC develops a peak at very low temperature.

In Fig. 3.14 we plot PC vs. temperature in the presence of RSO interaction for $g_1 = 0.5$ and compare with the graph for $g_1 = 0$. It is evidently clear that in the presence the electron-phonon interaction, the peak in PC becomes sharper and acquires a larger value.

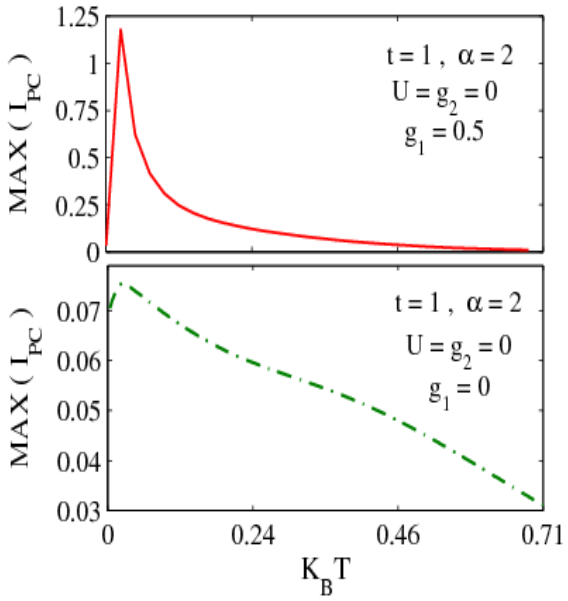

Fig. 3.14 I_{pc} as a function of temperature for different values of g_1 with $\alpha = 2$.

3.3.4 Effect of chemical potential

Finally, we wish to study the effect of chemical potential μ on PC. We put all the interactions equal to zero and for convenience, we all keep $K_BT = 0$ in all the four cases. In Fig. 3.15, we plot PC as a function of Φ for different values of μ. As expected, the magnitude and the phase of PC change with μ. The direct dependence of PC on μ is shown in Fig. 3.16 both in the presence and absence of the RSO interaction. In both cases, PC decreases with increasing μ, the values of PC being greater for the $\alpha = 2$ case.

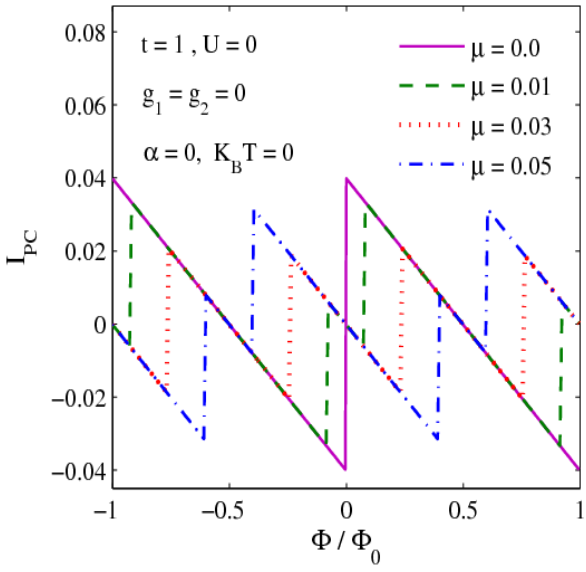

Fig. 3.15 I_{PC} vs. Φ for different values of μ.

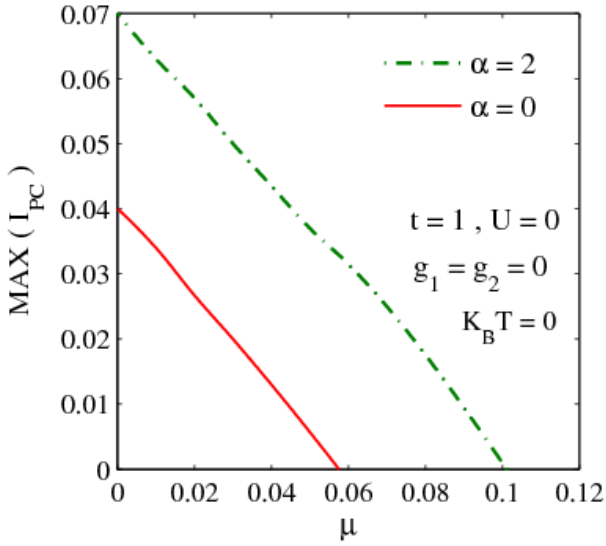

Fig. 3.16 PC vs μ for $\alpha = 2$ and $\alpha = 0$.

3.4 Conclusions

In this chapter, the effect of RSO interaction on PC is studied in a 1D HH ring threaded by an AB flux. First, the phonon degrees of freedom are eliminated by performing the conventional LFT and then the spin-dependence is removed by performing another unitary transformation. The effective electronic Hamiltonian is finally diagonalized by using a mean-field Hartree-Fock approximation and PC is calculated by differentiating the GS energy with respect to the flux. We show that the magnitude of PC is enhanced as we switch on the RSO interaction α. Also, for large values of α ($\alpha > 1$), the phase of PC is observed to change. We notice that both the electron-electron and electron-phonon interactions reduce the value of PC. We also observe that the NN electron-phonon interaction has a stronger

effect on PC than the on-site electron-phonon interaction has. We furthermore show that PC decreases with temperature and in the presence of electron-phonon interaction develops a sharp peak at low temperature. We finally show that the magnitude of PC decreases with increasing chemical potential and its phase also changes (as the number of particles change).

References

[1] M. Büttiker, Y. Imry and R. Landauer, *Phys. Lett. A* **96**, 365 (1983).

[2] H.-F. Cheung, Y. Gefen, E. K. Riedel and W.-H. Shih, *Phys. Rev. B* **37**, 6050 (1988).

[3] B. L. Altshuler, Y. Gefen and Y. Imry, *Phys. Rev. Lett.* **66**, 88 (1991);
F. von Oppen and E. K. Riedel, *Phys. Rev. Lett*. **66**, 84 (1991);
M. Abraham and R. Berkovits, *Phys. Rev. Lett.* **70**, 1509 (1993);
T. Giamarchi and B. S Shastry, *Phys. Rev. B* **5**, 10915 (1995);
L. K. Castelano, G. Q Hai, B. Partoens and F. M. Peeters, *Phys. Rev. B* **78**, 195315 (2008).

[4] L. P. Levy, G. Dolan, J. Dunsmuir, H. Bouchiat, *Phys. Rev. Lett.* **64**, 2074 (1990);
V. Chadrasekhar *et al*.**,** *Phys. Rev. Lett* **67**, 3578 (1991).

[5] G.Timp *et al*. , *Phys. Rev. B* **39**, 6227 (1991);
D. Mailly, C. Chapelier and A. Benoit, *Phys. Rev. Lett.* **70**, 2020 (1993);
J. Liu, K. Ismail, K. Y Lee, J. M Hong and S. Washburn, *Phys. Rev. B* **48**, 15148 (1993);
E. M. Q. Jariwala, P. Mohanty, M. B. Ketchen, R. A. Webb, *Phys. Rev. Lett.* **86**, 1594 (2001);

R. Deblock, R. Bel, B. Reulet, H. Bouchiat and D. Mailly, *Phys. Rev. Lett.* **89**, 206803 (2002).

[6] S. Viefers, P. Koskinen, P. Singha Deo and M. Manninen, *Physica E* **21**, 1-35 (2004).

[7] S. Gupta, S. Sil and B. Bhattacharyya, *Phys. Lett. A* **324**, 494 (2004);
S. K. Maiti, J. Chowdhury and S. N. Karmakar, *Phys. Lett. A* **332**, 497 (2004);
B.-B. Wei, S.-J. Gu and H.-Q. Lin, *J. Phys.: Condens. Matter* **20**, 395209 (2008);
S. K. Maiti, *Solid State Commun.* **150**, 2212 (2010).

[8] A. N Das and S. Sil, *J. Phys.: Condens. Matter* **5**, 8265 (1993);
Y. Takada and A. Chatterjee, *Phys. Rev. B* **67**, 081102 (R) (2003).

[9] T. Koga, J. Nitta, T. Akazaki and H. Takayanagi, *Phys. Rev. Lett.* **89**, 046801 (2002);
J. Premper, M. Trautmann, J. Henk and P. Bruno, *Phys. Rev. B* **76**, 073310 (2007);
S. Sil, S. K. Maiti and A. Chakrabarti, *J. Appl. Phys.* **112**, 024321 (2012);
S. K. Maiti, Moumita Dey, S. Sil, A. Chakrabarti and S. N. Karmakar, *Europhys. Lett.* **95**, 57008 (2011)

[10] S. Bellucci and P. Onorato, *Phys. Rev. B* **78**, 235312 (2008).

[11] M. Büttiker, *Phys. Rev. B* **32**, 1846 (1985).

[12] I. Lang and Y.A. Firsov, *Sov. Phys. JETP* **16**, 1301 (1963).

[13] D. Cabib and E. Callen, *Phys. Rev. B* **12**, 5249 (1975).

[14] W. Kohn, *Phys. Rev.* **133**, A171 (1964).

Chapter 4

The pinning effect in a Gaussian quantum dot: An improved Wigner-Brillouin perturbation theory approach

4.1 Introduction

Quantum dots (QD's) are ultra-low-dimensional structures with quantum confinement in all the spatial directions. As mentioned in Chapter 1, early experiments together with the generalized Kohn theorem predicted the nature of the confining potential in a QD to be parabolic. Consequently, extensive investigations have been carried out on QD's during the last three decades using the parabolic confinement potential (PCP) model. A huge amount of literature [1] has indeed piled up on this subject. However, we have also pointed out in Chapter 1 that more recent experiments have suggested that the confining potential in a QD to be anharmonic and in this context, the Gaussian confinement potential (GCP) model has turned out to be a particularly useful model [2]. We shall refer to a QD with GCP as a Gaussian QD (GQD) and that with PCP as a parabolic QD (PQD). Because of the realistic nature of the Gaussian potential, a good number of investigations have been reported in recent years on GQD's [3]. Of course, one can also use power law anharmonic potentials, but these potentials suffer from divergence syndrome at large distances, while the Gaussian

potential is by construction bound to give convergent results. One may, however, argue that in a QD the spatial coordinates never extend to a very large value to lead to any divergence problem, nevertheless, it is always appealing to work with a prescription that is mathematically sound and works in all limits.

The interaction of an electron with longitudinal optical (LO) phonons is known to play an important role on the electronic properties of semiconductor QD's [4] since the electron-phonon interaction energy scale is comparable to the other energies scales in such QD's. Many works have predicted the polaronic effects in polar semiconductor QD's [5]. One of the challenges in this context has been to suggest polaronic properties that could be measured so that the existence or otherwise of the polaronic effect in a QD can be verified experimentally. In an endeavor to achieve this goal, Mukhopadhyay and Chatterjee have studied the phonon-induced Zeeman splitting in a polar semiconductor QD [6]. Krishna et al. [7] have studied the optical absorption and oscillator strength of a QD. The polaronic effect has been studied in general by Yanar et al. [8] in GQD. One of the effects of polaronic interactions that can be observed experimentally is the pinning effect. Mukhopadhyay and Peeters have studied the so called "pinning effect" in a parabolic QD (PQD) [9].

4.1.1 Pinning Effect

In bulk polar semiconductors in a magnetic field, the first excited state (ES) Landau level plus a zero-phonon state is degenerate with the ground state (GS) Landau level plus one LO-phonon state at $\omega_0 = \omega_c$, where ω_0 is the LO-phonon frequency and ω_c is the cyclotron frequency. In the

presence of electron-phonon interaction, this degeneracy is lifted and if the magnetic field is sufficiently large, the first ES Landau level bends downward and asymptotically approaches the GS Landau level plus one LO-phonon energy. This is known as the pinning effect. In bulk polar systems, the splitting and pinning of the Landau levels in the presence of a magnetic field had been observed experimentally in the sixties [10]. Since a magnetic field provides an effective parabolic potential for the electron, a PQD is expected to show the pinning effect even in the absence of a magnetic field. This has been precisely shown by Mukhopadhyay and Peeters [9]. Since the Gaussian potential is a more realistic confining potential, it would be more appropriate to study the pinning effect in a GQD. Thus the study of pinning effect in a QD would be important both for the determination of the confinement potential and for the direct observation of the polaronic effect in QD's. The purpose of the present chapter is to investigate the pinning effect in a GQD in two-dimensions using the improved Wigner-Brillouin perturbation theory (IWBPT). Since GQD has two parameters to play with, namely the depth and the range, one would expect much richer pinning behavior in the case of a GQD. We finally apply our calculations to GaAs and InSb QD's.

4.2 The Model Hamiltonian and its Solution

The Hamiltonian of an electron moving in a GQD and interacting with the LO phonons of frequency ω_0 is given by

$$H' = \frac{\boldsymbol{p}'^2}{2m^*} + V'(\boldsymbol{\rho}') + \hbar\omega_0 \sum_{\boldsymbol{q}'} b^+_{\boldsymbol{q}'} b_{\boldsymbol{q}'} + \sum_{\boldsymbol{q}'} \left(\xi'_{\boldsymbol{q}'} e^{-i\boldsymbol{q}'\cdot\boldsymbol{\rho}} b^+_{\boldsymbol{q}'} + h.c \right) \qquad (4.1)$$

where all the vectors are two-dimensional (2D). In Eqn. (4.1), the first term is the electron kinetic energy with $\boldsymbol{p}'$ as the momentum operator the electron and m^* its effective mass, the second term is the confinement potential which we take as

$$V'(\boldsymbol{\rho}') = -V_0' \, e^{-\rho'^2/2R'^2} \ , \tag{4.2}$$

where $\boldsymbol{\rho}'$ is the position vector of the electron, V_0' the depth and R' the range of the potential, the third term is the phonon Hamiltonian, $b_{\boldsymbol{q}'}^{+}(b_{\boldsymbol{q}'})$ being the creation (annihilation) operator of a phonon of wave vector $\boldsymbol{q}'$ with dispersionless frequency ω_0 and the fourth term is the electron-phonon interaction with $\xi_{\boldsymbol{q}'}'$ as the electron-phonon interaction coefficient. We shall work in the Feynman units [8] in which the energy is scaled by the phonon energy $\hbar\omega_0$, length by the weak-coupling polaron radius, $r_0 = (\hbar/m^*\omega_0)^{1/2}$ and the wave vector by $q_0 = 1/r_0$. This is equivalent to putting $\hbar = m^* = \omega_0 = 1$. In these units, the dimensionless Hamiltonian reads as:

$$H = \frac{H'}{\hbar\omega_0} = \frac{\boldsymbol{p}^2}{2} \ - \ V_0 \, e^{-\rho^2/2R^2} + \sum_{\boldsymbol{q}} b_{\boldsymbol{q}}^{+} b_{\boldsymbol{q}} + \sum_{\boldsymbol{q}} \left(\xi_{\boldsymbol{q}} \, e^{-i\boldsymbol{q}.\boldsymbol{\rho}} \, b_{\boldsymbol{q}}^{+} + h.c \right), \tag{4.3}$$

where everything is dimensionless, $\boldsymbol{\rho} = \boldsymbol{\rho}'/r_0$, $\boldsymbol{q} = \boldsymbol{q}'/q_0$, $\boldsymbol{p} = \boldsymbol{p}'/\hbar q_0$, $V_0 = V_0'/\hbar\omega_0$, $R = R'/r_0$ and $\xi_{\boldsymbol{q}} = \xi_{\boldsymbol{q}'}'/\hbar\omega_0 = \left(\sqrt{2}\,\pi\alpha/vq\right)^{1/2}$, where v is the dimensionless volume in two-dimensions and α is the dimensionless electron-phonon coupling constant.

To make progress, we consider the Gaussian potential as a parabolic potential plus a perturbation. It is reasonable to make such an assumption

since the deviation of the Gaussian potential from the parabolic potential would be very small for small values of r. So we rewrite the Hamiltonian Eqn.(4.3) as

$$H = H_0 + H_1 + H_2 \ , \tag{4.4}$$

where

$$H_0 = \frac{\boldsymbol{p}^2}{2} + \left[\frac{1}{2}\omega_h^2\rho^2 - V_0\right] + \sum_{\boldsymbol{q}} b_{\boldsymbol{q}}^{+} b_{\boldsymbol{q}} \ , \tag{4.5}$$

$$H_1 = -\lambda\left[\frac{1}{2}\omega_h^2\rho^2 + V_0\left(e^{-\rho^2/2R^2} - 1\right)\right], \tag{4.6}$$

$$H_2 = \sum_{\boldsymbol{q}}\left(\xi_q\, e^{-i\boldsymbol{q}.\boldsymbol{\rho}}\, b_{\boldsymbol{q}}^{+} + h.c\right), \tag{4.7}$$

where $\lambda = 0$ for PQD, $\lambda = 1$ for GQD, $\omega_h^2 = V_0^2/R^2$, and H_1 and H_2 are the perturbations. We include the contribution from H_1 within the mean-field approximation (MFA) as:

$$H_1 = \lambda\left[\frac{V_0}{\langle\rho^2\rangle} - \frac{1}{2}\omega_h^2 - V_0\frac{\langle\, e^{-\rho^2/2R^2}\rangle}{\langle\rho^2\rangle}\right]\rho^2 , \tag{4.8}$$

where the expectation values are calculated with respect to the GS wave function (Ψ_{GS}) of the space part of the unperturbed harmonic oscillator Hamiltonian with frequency ω_h i.e., $\Psi_{GS} = (\omega_h/\pi)^{1/2}\exp(-\omega_h\rho^2/2)$. With this Ψ_{GS} we obtain,

$$\langle\rho^2\rangle = \frac{1}{\omega_h} \ , \tag{4.9}$$

and

$$\langle e^{-\rho^2/2R^2}\rangle = 2\omega_h R^2(1+2\omega_h R^2)^{-1} \ . \qquad (4.10)$$

The total Hamiltonian then reads

$$H = \frac{\boldsymbol{p}^2}{2} + \frac{1}{2}\omega^2\rho^2 - V_0 + \sum_q b_q^+ b_q + \sum_q \left(\xi_q \, e^{-i\boldsymbol{q}.\boldsymbol{\rho}} \, b_q^+ + h.c\right), \qquad (4.11)$$

with the effective harmonic confinement frequency

$$\omega = [(1-\lambda)\omega_h^2 + 2\lambda V_0\omega_h\{1-2\omega_h R^2(1+2\omega_h R^2)^{-1}\}]^{1/2} \ , \qquad (4.12)$$

which is actually $\frac{\omega'}{\omega_0}$, where ω' is the effective confinement frequency in actual units. The effective unperturbed energy (in Feynman units) is thus given by:

$$E^0_{j_1,j_2} = (j_1 + j_2 + 1)\omega - V_0 \qquad (4.13)$$

and we write the total energy corresponding to H as : $E_n = E_n{}'/\hbar\omega_0$, where $E_n{}'$ is the energy in actual units and E_n is the energy in Feynman units. We shall study the effect of H_2 using the perturbation theory and calculate the correction ΔE_n to the effective unperturbed electronic energy. Because of the presence of degeneracy in our problem, we need to use a degenerate perturbation theory and we shall employ the IWBPT [11]. The advantage with IWBPT is that it gives the correct pinning behaviour for weak electron-phonon interaction. The second-order correction to the unperturbed energy due to the electron-phonon interaction is given by

$$\Delta E_n = -\sum_j \sum_{\vec{q}} \frac{\left|\langle\varphi_j^0(\boldsymbol{\rho})|\xi_q e^{-i\boldsymbol{q}.\boldsymbol{\rho}}|\varphi_n^0(\boldsymbol{\rho})\rangle\right|^2}{E_j^0 - E_n^0 - \Delta_n + 1} \ , \qquad (4.14)$$

with $\Delta_n = \Delta E_n - \Delta E_0^{RSPT}$, where ΔE_0^{RSPT} is the Rayleigh–Schrödinger perturbation theory (RSPT) correction to the GS for the electron-phonon interaction and $\varphi_j^0(\vec{r})$ is the wave function of a harmonic oscillator with frequency ω. Since ΔE_n is present on the right hand side, we need to calculate the energy self-consistently. Eqn. (4.14) with $\Delta_n = 0$ gives the RSPT result which works well for the GS when $\omega \ll 1$. In Eqn. (4.14), if we put $\Delta_n = \Delta E_n$, that will be the case for Wigner-Brillouin Perturbation theory (WBPT) which can actually take care of the splitting of the degenerate energy levels. Eqn. (4.14) with $\Delta_n = \Delta E_n - \Delta E_0^{RSPT}$ is the case for IWBPT which gives the correct pinning effect.

To perform the summation in Eqn. (4.14), we use the following relation

$$\frac{1}{E_j^0 - E_n^0 - \Delta_n + 1} = \int_0^\infty e^{-\left(E_j^0 - E_n^0 - \Delta_n + 1\right)t}\, dt\,. \tag{4.15}$$

After simplifications, Eqn. (4.14) yields the energy corrections to the GS and the first two ES's as

$$-\frac{\Delta E_{GS}}{16\gamma} = B\left(\frac{1}{\omega}, \frac{1}{2}\right)\ , \tag{4.16}$$

$$-\frac{\Delta E_{1ES}}{4\gamma} = B\left(\frac{1-\Delta_1}{\omega} - 1, \frac{1}{2}\right) + 3\,B\left(\frac{1-\Delta_1}{\omega}, \frac{1}{2}\right)\ , \tag{4.17}$$

$$-\frac{\Delta E_{2ES}}{\gamma} = 5B\left(\frac{1-\Delta_2}{\omega} - 2, \frac{1}{2}\right) + 6B\left(\frac{1-\Delta_2}{\omega} - 1, \frac{1}{2}\right) + 13B\left(\frac{1-\Delta_2}{\omega}, \frac{1}{2}\right), \tag{4.18}$$

where $\gamma = [\alpha\sqrt{\pi}/32\sqrt{\omega}]$ and $B(x, y)$ is the beta function. In general, for an N-dimensional case the expressions are as follows:

$$-\frac{\Delta E_{GS}^{ND}}{8\beta} = B\left(\frac{1}{\omega},\frac{1}{2}\right) \quad , \tag{4.19}$$

$$-\frac{\Delta E_{1ES}^{ND}}{4\beta} = B\left(\frac{1-\Delta_1}{\omega}-1,\frac{1}{2}\right) + (2N-1)B\left(\frac{1-\Delta_1}{\omega},\frac{1}{2}\right) \quad , \tag{4.20}$$

$$-\frac{\Delta E_{2ES}^{ND}}{\beta} = (2N^2-4N+5)B\left(\frac{1-\Delta_2}{\omega}-2,\frac{1}{2}\right) + (4N-2)B\left(\frac{1-\Delta_2}{\omega}-1,\frac{1}{2}\right) + (2N^2+4N-3)B\left(\frac{1-\Delta_2}{\omega},\frac{1}{2}\right), \tag{4.21}$$

where

$$\beta = -\frac{\alpha}{32\sqrt{\omega}}\left[\frac{\Gamma\left(\frac{N-1}{2}\right)}{\Gamma\left(\frac{N}{2}+1\right)}\right]. \tag{4.22}$$

In the present problem, the region of interest is: $1-\Delta_n \cong n\omega$ and we consider the term which makes the maximum contribution to the energy in this region for each state ($n = 1,2,...$) and we obtain,

$$\Delta E_{1ES} = -\frac{\alpha\sqrt{\pi}}{8}\frac{\sqrt{\omega}}{1-\Delta_1-\omega}, \tag{4.23}$$

$$\Delta E_{2ES} = -\frac{5\alpha\sqrt{\pi}}{32}\frac{\sqrt{\omega}}{1-\Delta_2-2\omega} \ . \tag{4.24}$$

To see the pinning of the energy levels E_{1ES} and E_{2ES} to $[E_0^0+1$ phonon state], we have to consider the large ω limit. In this limiting case, a self-consistent calculation leads us to the following results:

$$E_{1ES} = \frac{N}{2}\omega + 1 + \Delta E_{GS} - \frac{\alpha\sqrt{\pi}\sqrt{\omega}}{8(\omega-1-\Delta E_{GS})}, \tag{4.25}$$

$$E_{2ES} = \frac{N}{2}\omega + 1 + \Delta E_{GS} - \frac{5\alpha\sqrt{\pi}\sqrt{\omega}}{32(2\omega - 1 - \Delta E_{GS})}\,. \qquad (4.26)$$

4.3 Numerical Details and Discussions

Our calculation is valid for any polar semiconductor QD. However, we shall apply our theory to GaAs and InSb QD's for the sake of concreteness. For GaAs, we take $\alpha = 0.07,\ \omega_0 = 5.5 \times 10^{13}/sec$ and $m^* = 0.6 \times 10^{-28} gm$ so that we have $\hbar\omega_0 = 36.25\ meV$ and $r_0 = 5.63\, nm$. Thus for GaAs, $V_0 = 0.4$ means: $0.4 \times \hbar\omega_0 = 14.5\, meV$ and $R = 3$ means: $3 \times r_0 = 16.9\, nm$. For InSb, we take $\alpha = 0.02,\ \omega_0 = 3.7 \times 10^{13}/sec$ and $m^* = 0.1279 \times 10^{-28} gm$ so that for InSb we have $\hbar\omega_0 = 24.38\, meV$ and $r_0 = 14.93\, nm$.

First of all, we notice that the relationship between the effective confinement frequency ω and the range of the Gaussian potential R is not so simple. In Fig 4.1, we plot ω vs. $1/\sqrt{R}$ for a GaAs QD and interestingly enough, the behaviour is almost linear unless R is extremely large. In this section, we shall always mean the confinement potential to be GCP unless otherwise mentioned.

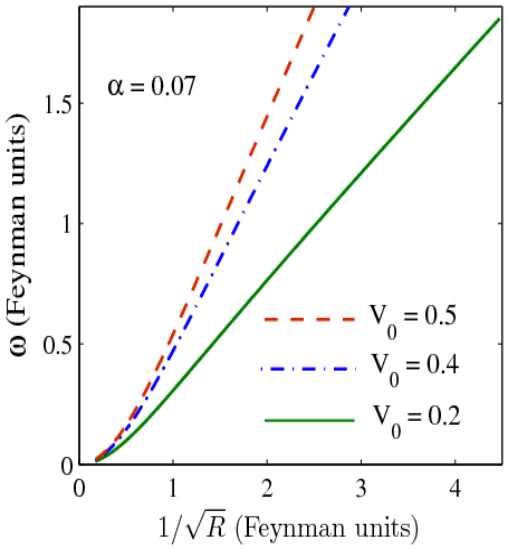

Fig. 4.1 ω vs. $1/\sqrt{R}$ for a GaAs QD for three values of V_0 .

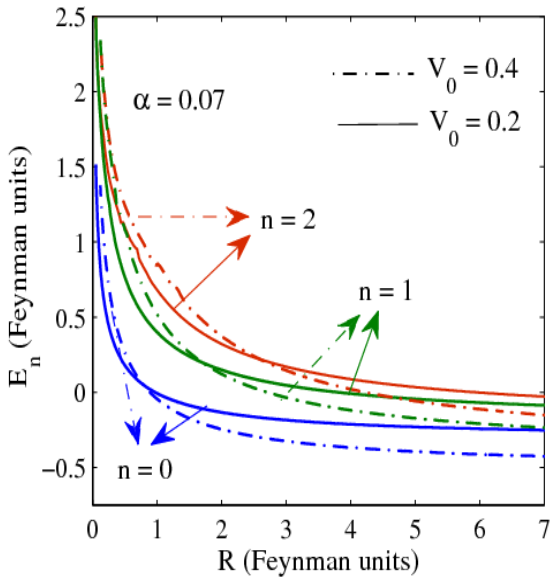

Fig. 4.2 GS and first two ES energies (E_0, E_1 and E_2) of a GaAs QD as a function of R for two values of V_0.

In Fig 4.2, we plot the GS and the first two ES energies (E_0, E_1 and E_2) of an electron confined in a GaAs QD as a function of the effective QD size R for two values of the depth of the Gaussian potential, V_0. For a particular value of V_0 and the electron-phonon coupling constant α, as R increases, energies decrease monotonically. However, at small values of R, as R increases, the energies decrease very rapidly for all the states and at large values of R, the energies decrease very slowly, ultimately saturating to the bulk limits.

When the QD size is small, the uncertainty in the momentum is expected to be large and as a result the kinetic energy itself will be large and hence the total energy increases as R decreases. Thus the polaronic effect is extremely significant for small QD's as has been predicted by a host of investigations [5]. It is also interesting to note that at small R, energies increase with increasing V_0, while above a certain QD size (which is different for different states), energies decrease with increasing V_0. This behavior can be roughly understood from the results of the finite square potential well problem. If the depth of the potential is V_0 and width of the well is R, then the GS energy can be written as $E_0 = V_0 cos^2(m^* R^2 E_0/2\hbar^2)$. When R is small, the kinetic energy is large and therefore E_0 can be approximated by the kinetic energy on the right hand side of the above equation and then as V_0 in increased, E_0 increases almost linearly. On the other hand, when R is large, the kinetic energy may be neglected and the particle can be expected to lie at the bottom of the potential well and so E_0 can be approximated by $[-V_0]$ on the right hand side of the above equation. In this case, as V_0 increases, E_0 decreases, at least for the parameter values considered in this work.

In Fig 4.3, we compare the energies of a GaAs QD obtained from the GCP and PCP models. It is clearly evident that the PCP model, in general, overestimates the energy. At large values of R, however, the results, as expected, become independent of the confinement potential models and consequently both the models give the same results which are, of course, the bulk limits.

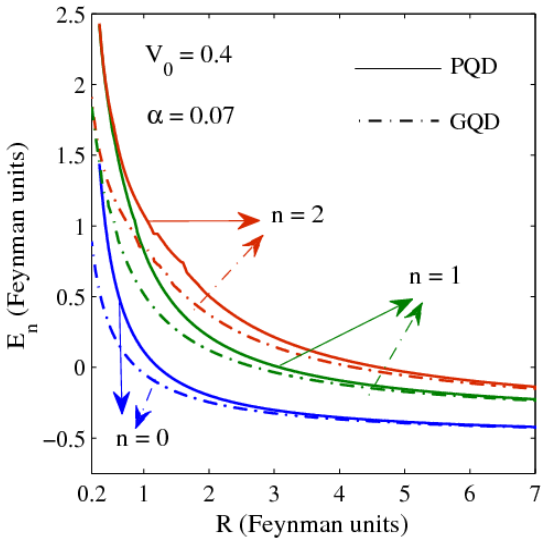

Fig. 4.3 Variation of E_0, E_1 and E_2 of a GaAs QD with GCP and PCP as a function of R for $V_0 = 0.4$.

In Fig. 4.4, we plot the energies of an electron confined in a GaAs QD as a function of ω both in the presence and absence of the electron-phonon interaction. The dashed-dotted lines represent the unperturbed energies and the solid lines indicate the energies of the electron when the electron-phonon interaction is taken into account. The unperturbed first and second electronic ES's plus zero-phonon are degenerate with the electronic GS plus one-phonon state at $\omega = 1$ and $\omega = 0.5$ respectively. In the presence of the

electron-phonon interaction, these degeneracies are lifted and the energy values are lowered. One can see from the figure that as ω approaches 1, the first ES energy (the solid curve) starts bending downward and with further

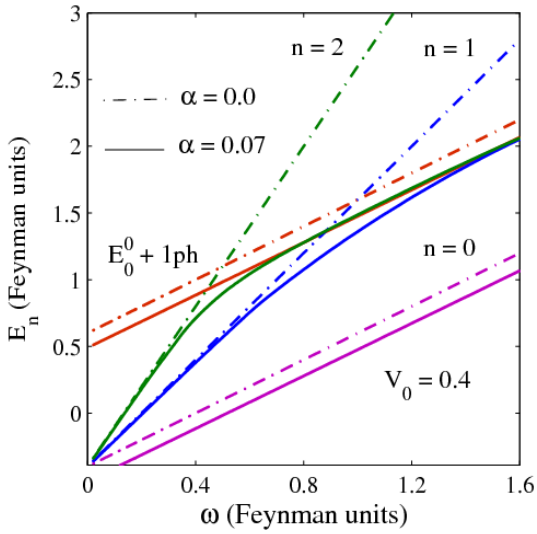

Fig. 4.4 E_0, E_1 and E_2 vs. ω for a GaAs QD with and without electron-phonon coupling for $V_0 = 0.4$

increase in ω gets pinned to the GS plus one-phonon energy. The removal of degeneracy by the electron-phonon interaction and the subsequent lowering of energy values are clear indications of the polaronic effects in a QD. Experimentally one should be able to observe the splitting and the pinning behavior of the energy levels and verify the existence of the polaronic effect in a QD.

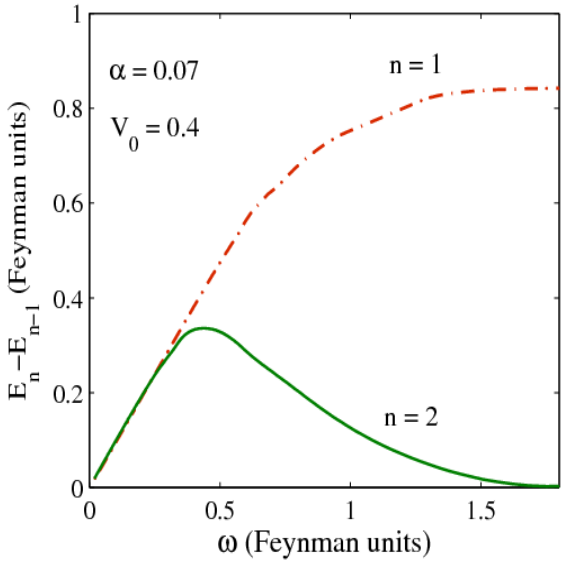

Fig 4.5: $\Delta E_{n,n-1}$ vs. ω for $n = 1$ and $n = 2$ for a GaAs QD with $V_0 = 0.4$.

In Fig 4.5, we plot $\Delta E_{n,n-1} = (E_n - E_{n-1})$ for $n = 1$ and $n = 2$ as a function of ω. ΔE_{10} seems to approach the one phonon energy as ω is increased, while ΔE_{21} initially increases, reaches a maximum and then decreases to zero under the same condition. This happens because in this limit, both the ES energies get pinned to the GS plus one-phonon energy.

In Fig 4.6, we plot E_0 , E_1 and E_2 of a GaAs QD as a function of $1/\sqrt{R}$ for $V_0 = 0.4$ and $V_0 = 0.2$ to see the effect of V_0 on the pinning effect. One can see that the degeneracies at two different values of R (for the two ES energies) are lifted and the energies are lowered in the presence of electron-phonon coupling. The pinning effect is also clearly visible. Experimentally, this might be a more direct and useful way of observing the pinning effect as compared to Fig. 4.3. It is interesting to observe that the pinning occurs for a lower value of ω as we increase V_0.

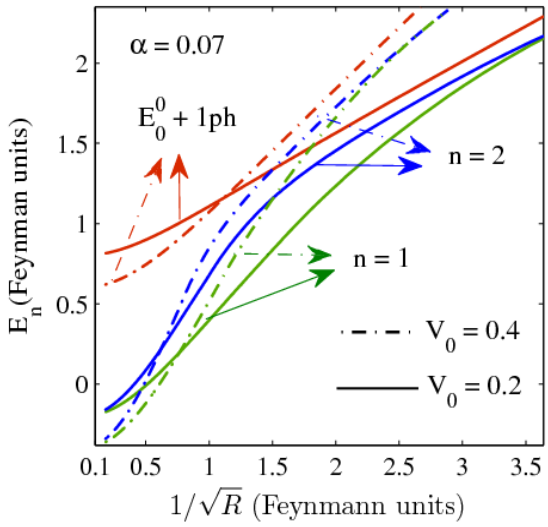

Fig. 4.6 E_1 and E_2 as a function of $1/\sqrt{R}$ for a GaAs QD for $V_0 = 0.4$ and 0.2.

In Fig. 4.7, we plot $(E_n - E_{n-1})$ as a function of $1/\sqrt{R}$, for $V_0 = 0.2$ and $V_0 = 0.4$. The behavior is more or less similar to that of Fig. 4.5. As

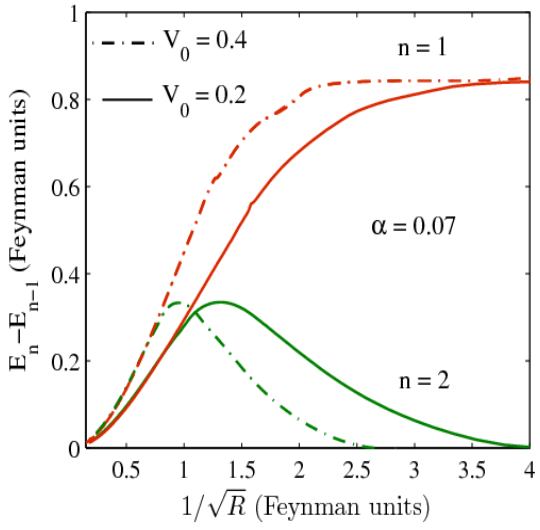

Fig. 4.7 $(E_2 - E_1)$ of a GaAs QD as a function of $1/\sqrt{R}$ for $V_0 = 0.2$ and 0.4.

R is reduced, $(E_2 - E_1)$ saturates to a constant which is expected to be a LO phonon energy in an ideal case and $(E_1 - E_0)$ goes through a maximum and finally reduces to zero. The reason for this behavior has already been explained earlier.

Fig. 4.8 shows the comparison of electronic energies as a function of ω' for GaAs and InSb QD's. For GaAs, the energy levels bend more and consequently the reduction in the energy values becomes more pronounced. Also the pinning occurs at a higher value of ω'. This becomes even more evident from Fig. 4.9 where we have plotted $(E'_n - E'_{n-1})$ as a function of ω'.

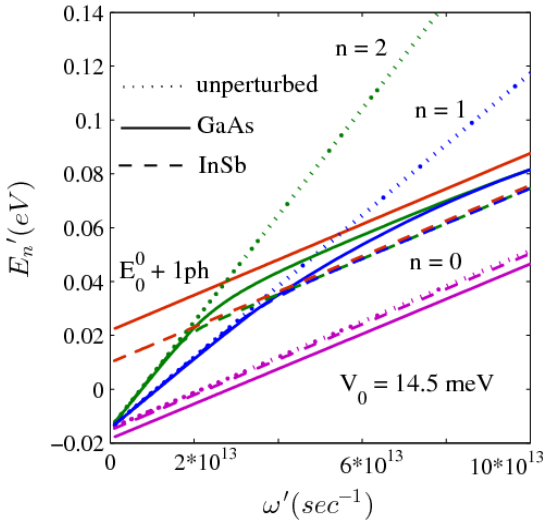

Fig. 4.8 E_0', E_1' and E_2' vs. ω' for GaAs and InSb QD's.

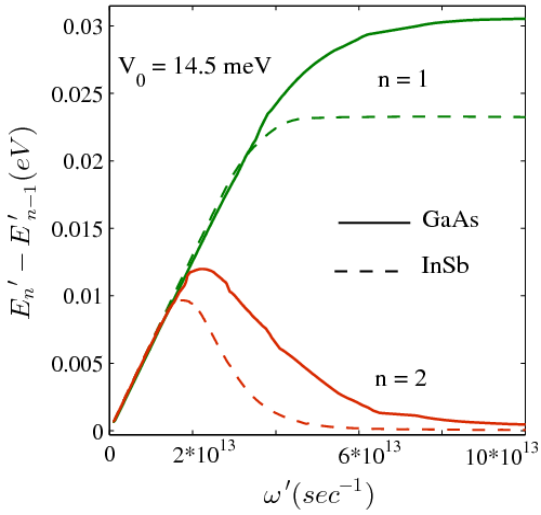

Fig. 4.9 $(E_n^{'} - E_{n-1}^{'})$ as a function of $\omega^{'}$ for GaAs and InSb QD's.

In Fig. 4.10, we have compared the pinning behavior in a GaAs QD as a function of $1/\sqrt{R}$ with both GCP and PCP models. As we can see from the figure, the pinning occurs at a larger ω value for the GCP model.

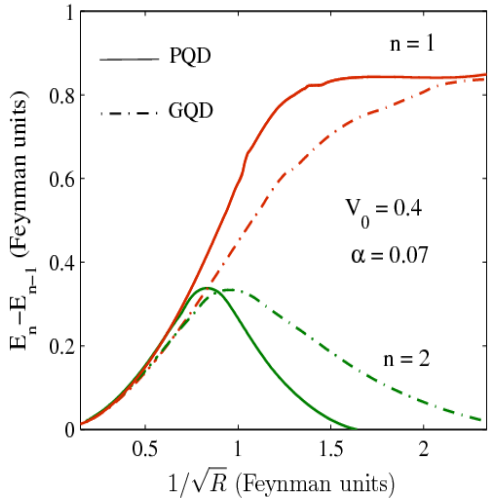

Fig. 4.10 The energy difference as a function of $1/\sqrt{R}$ for PQD and GQD of GaAs.

4.4 Conclusions

We have studied the effect of electron-phonon interaction on a few low-lying energy levels in a QD with GCP model and applied our results to GaAs and InSb QD's. We have particularly addressed ourselves to one of the most important polaronic effects called the pinning effect. We have shown that as the effective size, R of the QD is decreased, at certain R the degeneracies in the energy levels are lifted because of the electron-phonon interaction giving rise to splitting in the energy levels and the energy levels are shifted down. With the further reduction in the QD size, bending of the energies causes the ES levels to get pinned to the GS plus one-phonon energy. As the electron-phonon interaction is increased, the bending of the energy levels becomes more pronounced and the energy levels are further shifted down and pinning occurs at a larger value of the QD size. This splitting and pinning can be observed in the laboratory and the existence or otherwise of the polaronic effect in a polar QD can be tested experimentally. We have also studied the effect of the strength of the GCP, V_0 on the pinning effect. We find that as V_0 increases, pinning occurs at larger values of R. Also it turns out that the pinning takes place at a smaller confinement length in the case of a GQD as compared to that in a PQD.

References

[1] P. Moriarty, *Rep. Prog. Phys.* **64**, 297 (2001);
M. A .Kastner, *Rev. Mod. Phys.* **64**, 849 (1992);
N. F. Johnson, *J. Phys.: Condens. Matter* **7**, 965 (1995);
R. C. Ashoori, *Nature* **379**, 413 (1996);

U. Woggon, *Optical properties of Semiconductor Quantum Dots* (Springer, Berlin, 1997);

D. Bimberg, M. Grundmann and N. N. Ledentsov, *Quantum Dot Heterostructures* (Wiley, New York,1998);

F. Geerinckx, F. M. Peeters and J. T. Devreese, *J. Appl. Phys.* **68**, 3435 (1990);

J.-L. Zhu, J.-J. Xiong and B.-L. Gu, *Phys. Rev. B* **41**, 6001(1990);

T. Takagahara, *Phys. Rev. B* **47**, 4569 (1993);

N. Porras-Montenegro, S. T. Perez-Merchancano and A. Latge, *J. Appl. Phys.***74**, 7624 (1993);

J. L. Marín, R. Riera and S. A. Cruz, *J. Phys.: Condens. Matter* **10**, 1349 (1998);

Ch. Sikorski, U. Merkt, *Phys. Rev. Lett.* 62 (1989) 2164; *ibid. Surf. Sci.* **229**, 282 (1990);

B. Meurer, D. Heitmann, K. Ploog, *Phys. Rev. Lett.* **68**, 1371 (1992);

R. C. Ashoori *et al.*, *Phys. Rev. Lett.* **68**, 3088 (1992);

H. Drexler *et al.*, *Phys. Rev. Lett.* **73**, 2252 (1994).

[2] N. Bessis, G. Bessis and B. Joulakian, *J. Phys. A: Math. Gen.* **15**, 3679 (1982);

C. S. Lai, *J. Phys. A: Math. Gen.* **16**, L181 (1983);

R. E. Crandall, *J. Phys. A: Math. Gen.* **16**, L395 (1983);

M. Cohen, *J. Phys. A: Math. Gen.* **17**, L101 (1984);

A. Chatterjee, *J. Phys. A: Math. Gen.* **18**, 2403 (1985);

A. Chatterjee, *Phys. Rep.* **186**, 249 (1990).

[3] T. Sako, P.-A. Hervieux and G. H. F. Diercksen, *Phys. Rev. B* **74**, 045329 (2006);

W. Xie, *Solid State Commun.* **127**, 401 (2003);

B. Boyacioglu, M. Saglam and A. Chatterjee, *J. Phys. Condens.Matter* **19**, 456217 (2007);

S. S. Gomez and R. H. Romero, *Cent. Eur. J. Phys.* **7**, 12 (2009);

B. Boyacioglu and A. Chatterjee, *Int. J. Mod. Phys. B* **26**, 1250018 (2012).

[4] O. Verzelen, R. Ferreira and G. Bastard, *Phys. Rev. B* **64**, 075315 (2001);

T. Inoshita and H. Sakaki, *Phys. Rev. B* **56**, R4355-R4358 (1997);

M. A. Odnoblyudov, I. N. Yassievich and K. A. Chao, *Phys. Rev. Lett.* **83**, 4884 (1999);

L. Jacakl, J. Krasnyj, D. Jacak and P. Machnikowski, *Phys. Rev. B* **65,** 113305 (2002).

[5] M. H. Degani and G. A. Farias, *Phys. Rev. B* **42**, 11950 (1990);

L. Wendler, A. V. Chaplik, R. Haupt and O.Hipolito, *J. Phys. Condens. Matter* **5**, 8031 (1993);

K. D. Zhu and S. W. Gu, *Phys. Rev. B* **47**, 12947 (1993);

K. D. Zhu and T. Kobayashi, *Solid State Commun.* **92**, 353 (1994);

S. Mukhopadhyay and A.Chatterjee, *Phys.Lett. A* **204**, 411 (1995);

S. Mukhopadhyay and A. Chatterjee, *Phys. Rev. B* **55**, 9297 (1997);

C. Y. Chen, P. W. Jin, W. S. Li and D. L. Din, *Phys. Rev*. **56**, 14913 (1997);

S. Mukhopadhyay and A. Chatterjee, *Phys. Rev. B* **58**, 2088 (1998);

S. Mukhopadhyay and A. Chatterjee, *Phys. Lett. A* **240**, 100 (1998);

S. Mukhopadhyay and A. Chatterjee, *J. Phys.: Condens. Matter* **11**, 2071 (1999);

M. A. Odnoblyudov, I. N. Yassievich and K. A. Chao, *Phys. Rev.Lett.* **83,** 4884 (1999);

N. Kervan, T. Altanhan and A. Chatterjee, *Phys. Lett. A* **315**, 280

(2003);

P. M. Krishna and A. Chatterjee, *Physica E* **30**, 64 (2005);

P. M. Krishna, S. Mukhopadhyay and A. Chatterjee, *Phys. Lett. A* **360**, 655 (2007).

[6] S. Mukhopadhyay and A. Chatterjee, *Phys. Rev. B* **59**, R7833 (1999);

S. Mukhopadhyay and A. Chatterjee, *Int. J. Mod. Phys. B* **14**, 3897 (2000);

S. Mukhopadhyay, B. Boyacioglu, M. Saglam and A. Chatterjee, *Physica E* **40**, 2776-2782 (2008).

[7] P. M. Krishna, S. Mukhopadhyay and A. Chatterjee , *Int. J. Mod. Phys. B* **16**, 1489 (2002).

[8] S. Yanar *et al.*, *Superlattices and Microstruct.* **43**, 208 (2008).

[9] S. Mukhopadhyay and F. M. Peeters, *J. Phys.: Condens. Matter* **14,** 8005-8010 (2002).

[10] E. J. Johnson and D. M. Larsen, *Phys. Rev.Lett.***16**, 655 (1966);

D. H. Dickey, E.J. Johnson and D.M Larsen, *Phys. Rev. Lett.***18**, 599 (1967);

G. Lindemann, R. Lassing, W. Seidenbusch and E. Gornik, *Phys. Rev. B* **28**, 4693 (1983).

[11] F. M. Peeters and J. T. Devreese, *Phys. Rev. B* **31**, 3689 (1985);

G.Q. Hai, F.M. Peeters and J.T. Devreese, *Physica B* **184**, 289 (1993);

F. A. P. Osorio, Marcelo Z. Maialle and O. Hipolito, *Phys. Rev. B* **57,** 1644 (1998);

I. Hubac and S. Wilson, *J. Phys. B: At. Mol. Opt. Phys.* **33**, 365–374 (2000).

Chapter 5

Conclusions

In this thesis we have investigated the effects of electron-phonon interaction in low-dimensional systems such as Luttinger liquids, Hubbard rings and quantum dots. We have begun the dissertation with an introductory chapter (Chapter 1) where we have presented a general introduction to the various systems we have studied in this thesis.

In Chapter 2, we have considered the celebrated Luttinger model which is an exactly solvable model and is important from the point of view of understanding the electronic properties of one dimensional (1D) systems. The Luttinger-liquid behaviour has indeed been observed experimentally in carbon nanotubes and other quasi-one-dimensional organic solids such as TTF-TCNQ in which the conductivity is thought to be largely 1D. We have studied the fully interacting many electron-phonon problem within the framework of Luttinger model which we have termed as the *Fröhlich-Toyozawa-Luttinger* (FTL) liquid. The calculation of momentum distribution function can prove to be very important in understanding many interesting properties of one-dimensional strongly correlated systems. We have obtained an exact analytical expression for the electron momentum distribution function of the Fr*ö*hlich-Toyozawa-Luttinger (FTL) liquid. It is well-known that if there is no interaction, a sharp Fermi surface exists and as we turn on the interaction it starts disappearing. Lieb and Mattis have found that in a Luttinger liquid the Coulomb interactions removes the discontinuity but, there still exists a *residual Fermi surface* at $k = k_F$. We

have shown that strong Coulomb interactions completely destroy the residual Fermi surface of a Luttinger liquid. We have also shown that in the case of an FTL liquid, the residual Fermi surface is also destroyed by the electron-phonon interactions. Furthermore, the optical-phonon interaction is observed to have a larger effect on the distribution function than the acoustic-phonon interaction. It has also been observed that the distribution function has a very long tail above k_F in an FTL liquid, which is in fact unaffected by the strengths of the electron-electron and electron-phonon interactions. Thus the momentum distribution function of an FTL liquid shows a qualitatively different behaviour from that of a Luttinger liquid above k_F particularly for low-lying excitations.

Next, we have considered a correlated quantum ring (QR) threaded by an Aharonov-Bohm (AB) flux and looked into the effects of Rashba spin-orbit (RSO) interactions on the persistent current (PC) in this ring in the presence of electron-phonon interaction. The Rashba interaction is important because it can be controlled by tuning the external electric field which is exactly the idea behind spintronics. We have modeled the quantum ring by the Holstein-Hubbard-Rashba Hamiltonian and calculated the energy. First, we have eliminated the phonon degrees of freedom by performing the conventional Lang-Firsov transformation and then the spin-dependence has been eliminated by using another unitary transformation. The effective electronic Hamiltonian is finally diagonalized by using a mean-field Hartree-Fock approximation and PC has been calculated by differentiating the ground state (GS) energy with respect to the flux. We have shown that the magnitude of PC is enhanced as we switch on the RSO interaction (measured by the strength α). Also, for large values of α ($\alpha > 1$), the phase of PC is observed to change. We have shown that both the

electron-electron and electron-phonon interactions reduce the value of PC. We have also shown that the nearest-neighbour electron-phonon interaction has a stronger effect on PC than the onsite electron-phonon interaction has. In addition to this, we have shown that PC decreases with temperature and the PC curve becomes smoother with temperature. It is found that in the presence of electron-phonon interaction PC develops a sharp peak at low temperature. We have furthermore observed that the number of electrons in a QR can also change the magnitude and phase of the PC and therefore the chemical potential is expected to have a significant effect on PC. We have shown that the magnitude of PC decreases with increasing chemical potential and its phase also changes as the number of particles change.

Finally, we have studied the effect of electron-phonon interaction on a few low-lying energy levels in a QD with Gaussian confinement. We have particularly studied the pinning effect using the improved Wigner-Brillouin perturbation theory (IWBPT). We have shown that as the effective size, R of the QD is decreased, at certain R the degeneracies in the energy levels are lifted because of the electron-phonon interaction giving rise to splitting in the energy levels and the energy levels are shifted down. With the further reduction in the QD size, bending of the energies causes the ES's to get pinned to the GS plus one-phonon energy. As the electron-phonon interaction is increased, the bending of the energy levels becomes more pronounced and the energy levels are further shifted down and pinning occurs at a larger value of the QD size. This splitting and pinning can be observed in the laboratory and the existence of the polaronic effect in a polar QD can be tested experimentally. We have also studied the effect of the strength of the Gaussian confining potential, V_0 on the pinning effect. We find that as V_0 increases, pinning occurs at larger values of R. We have

compared the pinning effect in a GQD with that in a PQD. It turns out that the pinning takes place at a smaller confinement length in the case of a GQD as compared to that in a PQD. Finally, we have applied our results to GaAs and InSb QD's.

List of publications based on which the present thesis has been written

1. **Monisha P.J**, S. Mukhopadhyay and A. Chatterjee, "Exact distribution function of a one-dimensional Frohlich-Toyozawa-Luttinger Liquid", *Solid State Communications* ***166,*** 83-86 (2013).

2. **Monisha P.J** and S. Mukhopadhyay, "The Pinning effect in a Gaussian quantum dot: A study using the Improved Wigner-Brillouin Perturbation theory", *Physica B* **464**, 38–43 (2015).

3. **Monisha P.J**, I.V. Sankar, S. Sil and A. Chatterjee, "Persistent current in a correlated quantum ring with electron-phonon interaction in the presence of Rashba interaction and Aharonov-Bohm flux", *Scientific Reports* **6**, 20056 (2016).

Other publications

4. I.V. Sankar, **Monisha P.J**, S. Sil and A. Chatterjee, "Persistent current in the Holstein-Hubbard quantum ring", *Physica E* **73** ,175–180 (2015).

Publications in conference proceedings

1. **P.J Monisha**, Soma Mukhopadhyay and Ashok Chatterjee, "The momentum distribution function of a Luttinger liquid", *AIP Conference Proceedings* **1512**, 834 (2013).

2. **P.J Monisha** and Soma Mukhopadhyay "The Pinning Effect in Quantum Dots", *AIP Conference Proceedings* **1591**, 1135 (2014).

3. **Monisha P.J**, I.V. Sankar, S. Sil and A. Chatterjee, "Effects of Spin-Orbit Interaction on Persistent Current in a Nano Ring", *Materials Today: Proceedings* **2**, 4495 – 4498 (2015).